CHARACTERISTICS OF SOOT FORMATION AND BURNOUT IN TURBULENT RECIRCULATING FLAMES

By

ABDERRAHMANE TOUATI

A DISSERTATION PRESENTED TO THE GRADUATE SCHOOL
OF THE UNIVERSITY OF FLORIDA IN
PARTIAL FULFILLMENT OF THE REQUIREMENTS
FOR THE DEGREE OF DOCTOR OF PHILOSOPHY

UNIVERSITY OF FLORIDA

1987

DEDICATED TO MY PARENTS

ACKNOWLEDGMENT

The author would like to thank Dr. Charles L. Proctor II, chairman of the supervisory committee, for his valuable assistance in conducting this project. Special thanks are extended to Dr. Alex Green, Dr. Roger Gater, Dr. John Eyler, and Dr. William Lear for serving as committee members.

This research effort was conducted under a contract from the US Air Force, Tyndall Air Force Base, Environics Division, Panama City, Florida. The author would like to thank the personnel of the Environics Division for their support and friendship throughout the 2-1/2 years that he spent working with them. Special thanks are extended to Major Paul Kerch, Dr. Joe Wander, and MSgt. Dan Stork.

The author would like to acknowledge Dr. William Shultz and Ms. Mary McGill for chemical analyses of the soot samples, and Dr. Richard Irey and Dr. Art Sterling for valuable technical discussions.

Special thanks are extended to Mrs. Becky Hoover and her daughters Pam and Kim for their friendship and help in preparing this manuscript.

TABLE OF CONTENTS

		Page
ACKNOWLEDGMENT		iii
ABSTRACT		vi
CHAPTERS		
I	INTRODUCTION	1
II	SOOT FORMATION	7
	Introduction	7
	Soot Precursors	8
	Neutral Species Mechanisms	8
	Ionic Mechanisms	14
	Soot Emission Models	23
	Experimental Observations	30
III	EXPERIMENTAL METHODS	39
	Modular Burner	40
	Physical Sampling	43
	Temperature Probe	47
	Integrated Particle Sizing System	47
IV	EVALUATION OF THE OPTICAL SYSTEM	60
	Cold Flow	62
	Hot Flow	68
	Reproducibility of Soot Data	75
V	SOOT MORPHOLOGY AND CHEMICAL ANALYSIS OF PAHs ADSORBED ON THE SOOT PARTICLE SURFACE	77
	Morphology	77
	Chemical Analysis of PAHs Collected on the Soot Particle Surface	79
VI	EXPERIMENTAL RESULTS AND DISCUSSIONS	88
	Introduction	88
	Experimental Conditions	89
	Velocity Measurements	90
	Temperature Measurements	97
	Soot Measurements	112

VII CONCLUSIONS AND RECOMMENDATIONS 152

Conclusions 152
Recommendations..... 154

REFERENCES 155

BIOGRAPHICAL SKETCH 164

Abstract of Dissertation Presented to the Graduate School of the University of Florida in Partial Fulfillment of the Requirements for the Degree of Doctor of Philosophy

CHARACTERISTICS OF SOOT FORMATION AND BURNOUT IN TURBULENT RECIRCULATING FLAMES

By

ABDERRAHMANE TOUATI

August, 1987

Chairman: Charles L. Proctor, II
Major Department: Mechanical Engineering

The present study represents an investigation of the effect of fuel type, fuel stream heat content, nitrogen dilution, and air jet velocity on soot formation rates and particle burnout in a highly recirculating, turbulent-type flame. Soot particle size and flux measurements have been made using an optical probe based on a large angle ratioing technique to measure the intensity of forward scattered light from individual particles at two off-axis angles. Chemical analyses of soot samples have been made using a gas chromatograph with a flame ionization detector (FID), and a morphological analysis of soot samples has been made using a scanning electron microscope (SEM). Physical probes have been used for temperature measurements and extraction of soot particles.

Chemical analysis of the composition of the polycyclic aromatic hydrocarbons (PAHs) extracted from soot samples collected at the face of the burner and on a filter located downstream in the exhaust system suggests that multiple, convergent pathways, rather than one chemical mechanism, lead to the formation of high molecular weight PAHs and soot.

Net soot production was found to be the result of the competition of soot particle formation and burnout. The fuel type and the fuel stream heat content appear the main parameters that determine the flame's propensity to soot. The addition of nitrogen to a fuel stream increases the difference in the net soot production among the fuels investigated. Dilution by nitrogen decreases more effectively the oxidation rate of soot particles in flames that use fuels of lower heat content.

CHAPTER I
INTRODUCTION

Unburned hydrocarbon particles are detrimental both to human health and to the efficiency of fuel-powered engines. Both of these problems must be acknowledged by any program to develop technologies that would use fuels having a broader range of properties, which eventually would lead to increased soot emissions. The goal of modern engine designers is to devise combustors giving optimum performance while satisfying environmental quality requirements. Therefore, an understanding of soot formation and destruction in combustion chambers is a prerequisite for achievement of this goal.

Soot emissions involve several interactive processes that occur simultaneously in a combustion environment. Such processes include chemical and physical aspects of soot formation and growth, fluid mechanics involved in the transport of mass, momentum, and energy between different regions of the flames, and radiative heat transfer from the flame to the surroundings.

Researchers in this field continue to attempt to devise laboratory scale experiments that can decouple the different processes occurring in soot formation. For example, shock tubes and simple flames have been used to

examine the chemistry of formation of soot particles, and several theories based on neutral or/and ionic mechanisms have been proposed to describe the chemical processes associated with soot formation. These theories were based on experimental observations on the fate of gaseous products and particles in flames. To date, no theory has been universally accepted because of the complexity of the subject. These complexities result from the very fast rates of chemical reactions leading to soot formation and from the dependence of the relative rates of competing pathways leading to the formation of soot under varying experimental conditions.

Notwithstanding the importance of chemistry in understanding the incipience of soot particles, chemistry, alone, does not exclusively explain the formation of soot in flames. Such physical processes as particle growth, which accounts for most of the soot loading (Prado and Lahaye, 1981), and fluid mechanics are no less important than the chemical processes in understanding soot formation. Modeling all the processes that are involved in the formation and evolution of soot particles in flames requires an extensive database, which is not available at this time. Current limitations in state-of-the-art analytical techniques and in computer storage preclude detailed modeling of all the steps of soot formation.

Because of the complexities involved in developing a detailed phenomenological model of soot formation, only few predictive models for the rate of soot formation and consumption have been proposed. Most of the proposed models were based either on correlative equations dependent on experimental conditions but not on chemical kinetics of the system or on global or quasi-global kinetic concepts that use unrealistically simplified chemical kinetic equations. At the present time, the simplistic approach of these models generally affords more-satisfactory descriptions than do detailed approaches to the prediction of soot formation in a well defined combustor configuration; however, it must be recognized that development of models has been constrained by the paucity of detailed and accurate measurements of the fundamental chemical and physical parameters that control soot formation. Determining and elucidating the effects of these parameters on soot formation will contribute to a database for developing more efficient predictive models.

Experimental diagnostics on gas turbine engines can be very difficult and costly; therefore, gas turbine engines were not an attractive alternative to the simpler fundamental laboratory burners. A bluff body burner was used in this study to provide both reasonable simulation of the combustion process in gas turbine engines and simplicity of operation. Burners of this type, which were designed to provide an intermediate combustor for practical

studies (Roquemore et al., 1983), produce axisymmetrical turbulent flames that simulate a wide range of practical combustors.

Evaluation and development of models of soot formation and destruction are possible only after a) accurate characterization of species and particles as they exist in a realistic flame and b) determination of the fundamental parameters that control the different processes involved in the formation and destruction of soot. Accordingly, this investigation was designed to meet two main objectives, which can be described as follows: first, to evaluate the performance of an optical diagnostic system for both particle size and count rate measurements, with emphasis on characterization of soot particulates in combustion and to perform the necessary adjustments for optimization of data acquisition; second, to identify and assess the main parameters that control soot formation in well defined experiments.

The optical diagnostic systems used in this study consist of an Integrated Particle Sizing System (IPSS) for particle size and population density measurements. A thorough analysis of the IPSS was undertaken to evaluate its performance as a particle sizer and particle counting instrument in both reacting and non-reacting flows. Polystyrene latex spheres of known size were used to calibrate and verify the performance of the instrument in a

non-reacting medium. The system's response for size and particle count rate measurements in non-reacting and reacting flows assessed the viability of the instrument.

The aim of this work was to improve understanding of processes of soot formation and destruction by using state-of-the-art techniques to measure soot particle diameter and number density in conjunction with temperature and velocity profiles in a highly turbulent recirculating flame. Any change in the operating conditions of the combustors would strongly affect the formation and destruction rates of soot particles as well as the temperature and velocity profiles in the flames. The thrust of this work was to devise well conceived experiments to decouple the different processes that occur in combustion flames and determine the main parameters that control the soot formation and subsequently the oxidation rates of soot particles.

The formation and evolution of the soot particles in flames were argued to be strongly affected by the temperature history, residence time, and fuel structure (Santoro and Semerjian, 1985). Accordingly, detailed measurements of soot particle size and number density, temperature, and velocity were used to investigate the different processes involved in soot formation and burnout in a turbulent recirculating flame. Given the importance of mixing in turbulent recirculating flames, flowfield mapping was performed to localize the regions of greatest soot particle loading and to trace the mean path of soot particles through the flame.

Temperature, velocity, and species concentrations are interdependent state parameters that vary with the operating conditions. Their separate effects on soot formation can be examined by using a selective set of independent controlling parameters. The controlling parameters that were investigated in this study are fuel type, fuel flow rate, fuel heat content, and fuel and air jet velocities. Nitrogen dilution was used to control the fuel jet velocity and the fuel jet heat content.

A general overview on the work that has been accomplished in the area of soot formation will be given in chapter II. The experimental equipments used in this work will be described in chapter III, followed in chapter IV by a thorough analysis of the Integrated Particle Sizing System to evaluate its overall performance as a particle sizer as well as a particle counter. Soot morphology and chemical analysis of soot samples obtained from different flames will be covered in chapter V. The experimental results and discussion of this research effort will be presented in chapter VI. Finally, in chapter VII the main conclusions will be drawn and recommendations for future areas of research will be offered.

CHAPTER II
A GENERAL REVIEW OF SOOT FORMATION

Introduction

The soot formation process which occurs during combustion of hydrocarbon is yet to be understood by the community working in this field of research. Although several theories of soot formation have evolved over many years of research, none of them have been universally accepted because of the complexity of the subject. These theories historically were derived from experimental observations, and advances in determining their validity have only recently become possible through the development of new experimental techniques. These new techniques, which permit the study of molecular species and particles as they exist in flames, include mass spectrometry (Calcote, 1963; Michaud et al., 1981), laser light scattering (Kent et al., 1981; D´Alessio et al., 1977), laser induced fluorescence (DiLorenzo et al., 1981), laser-induced ionization (Smyth and Mallard, 1981) and other intrusive or non-intrusive techniques.

This chapter summarizes the work that has been accomplished in this field and justifies the experimental approach of this research program; it includes the proposed mechanisms leading to the formation of the first solid soot particles, recent experimental developments in the study of

soot formation in shock tubes and flames, and a review of some analytical/correlative models for soot emissions.

Soot Precursors

The primary soot particles formed in flames consist of spherical or near spherical elementary particles which have mean diameters in the range of 10-50 nanometers, and a carbon-hydrogen atom ratio in the range 8:1-12:1 (Calcote, 1981).

Soot forms in hydrocarbon flames by a succession of fast processes that occur within few milliseconds. In the first process, nucleation , embryonic gaseous species (soot precursors) undergo a series of gas phase reactions to form the first solid particles. In the second, surface growth, small solid particles coalesce to form large spherules. In the final process, the spherules aggregate to form chains.

Neutral Species Mechanisms

As attempts were made to develop comprehensive phenomenological models for soot formation, the combustion chemistry of neutral species in flames has given birth to new theories. The development of new experimental techniques for sampling species detected in flames has been very helpful in understanding soot phenomena. The new findings, however, have discredited many theories that had attempted to explain the principal routes leading to soot formation. Workers in the field of carbon formation in flames have failed to agree on a neutral species mechanism

that describes the phenomenological process of soot formation. No attempt will be made to discuss all the various theories because they have been reviewed by several authors such as Palmer and Cullis (1965), Gaydon and Wolfhard (1970) and others; however, the most recent viable neutral-species mechanisms, which have received support, will be discussed.

Homann and Wagner (1967, 1968) suggested that intermediate hydrocarbons have an acetylenic character that enables them to be added to other hydrocarbons and still retain their radical character. They argued that the rate of polyacetylene formation can be explained only by radical reactions and that the polyacetylenes are subsequently rearranged to an aromatic graphite-like structure and soot. This scheme was proposed based on their observations of the fate of the polyacetylenes and polycyclic aromatics in the oxidation region of the flames they studied. The concentration of polyacetylenes was observed to decrease while the concentration of the polycyclic aromatics was increasing in the oxidation region. From considerations of the results of other workers (Cullis et al., 1967), Bonne et al., 1965; Thomas, 1962), Calcote (1981) concluded that the cyclization process in the polyacetylene scheme would be too slow to account for the rapid formation of soot particles in the post oxidation zone. Further, the unfavorable thermochemistry of large C_nH and C_nH_2 species might explain the rapid decrease in their concentrations.

Homann and Wagner suggest the possibility of C_2H or other radicals attacking a polyacetylene molecule to give a branching radical with ring closure. The latter approach was been reinforced by the work of Crittenden and Long (1973) who concluded that an aromatic ring with a two-carbon side chain (i.e., C_6-C_2) can be formed from polyacetylene branch radicals by ring-closure or by cyclization. The latter species, still having radical character, will grow to small carbon particles as further polyacetylenes are added.

Glassman (1979) considered a model where both free radicals and ions have a role in the formation of incipient soot particles. He emphasized the importance of strongly conjugated molecules having resonance structures on the stability and reactivity requirements of soot formation. As pointed out by the author, such strongly conjugated molecules as butadiene and benzene undergo rapid reactions with each other, with ions, and with other neutral molecules and radicals. They are also stabilized by their polar resonance structure. Although butadiene has less resonance energy than benzene, its ability to accept a positive ion and form an even more reactive carbonium ion can make it the most likely precursor to nucleation. This can be seen in the following example:

$$H_2C{=}CH{-}CH{=}CH_2 + H^+ \longrightarrow \begin{matrix} CH_3{-}C & + & H{-}CH{=}CH_2 \\ \updownarrow & & \\ H_3{-}CH{=}C & + & H{=}CH_2 \end{matrix}$$

According to Glassman's model butadiene forms from acetylene in premixed flames, and probably reacts further to form larger precursor radicals, which undergo further addition and dehydration via a combination of reactions involving radical and ionic compounds. The products of these reactions, under the conceptual scheme developed by Glassman, undergo Diels--Alder cyclization leading to polynuclear aromatics. Another feature of butadiene, as noted by Glassman, is that of all the fuels tested, it has the greatest tendency to soot in a diffusion flame. The principal objection to the model is that the concentration of butadiene falls very rapidly even before soot particles are observed (Calcote, 1981).

Bittner and Howard (1981 a&b) reported mole-fraction profiles of stable and free radical species in a benzene-oxygen-argon flame near the sooting limit (equivalence ratio = 1.8). They concluded that PAH observed in sooting flames cannot be formed by condensation reactions of intact aromatic rings, and that much of the carbon that ends up as soot may come from non-aromatic hydrocarbon intermediates. Their flux profiles for C_6H_6 and C_2H_2 indicate that the reaction of OH, rather than O, with benzene may be the primary source of C_6H_6O, followed by production of CO and C_5H_6; however, acetylene is not an early product in the ring fragmentation.

A sequential mechanism is outlined by these workers for the production of C_1, C_2, C_3, C_4 ,and C_5 from benzene that is consistent with the flux profiles of intermediate species. They observed that as the fuel equivalence ratio is increased past the sooting limit, a sequential growth from polycyclic aromatic hydrocarbons of 120-210 daltons to heavier species occurs, and then soot is formed. They point out that rapid growth of aromatic structures by free-radical addition may result in a stabilization of the intermediate without formation of six-membered rings. Among the possible free-radical addition schemes proposed for PAH and soot formation, reaction of the phenyl radical (C_6H_5) with vinylacetylene has been found the most favorable for stabilizing the intermediate to form a six membered ring.

Stein (1978) suggested that concentration profiles of the most reactive species cannot, in themselves, explain the chemistry of polycyclic aromatic hydrocarbon (PAH) and soot formation. He conducted studies on the equilibrium behavior of PAHs in hydrocarbon systems at high temperatures to elucidate the chemical steps leading to their growth and finally to formation of soot particles. One important finding of his studies is that above 1700K, the concentration of highly condensed PAHs passes through a minimum. He concluded that since only highly condensed aromatic hydrocarbons (i.e., benzene, coronene,) are capable of extensive growth, this minimum may constitute an

effective thermodynamic barrier to formation of soot particles at high temperatures. A polymerization scheme is given below by the author for the first six members of the most thermodynamically favorable high-temperature polymerization route. In this scheme C_2 and C_4H_2 refer only to the number and type of atoms added in each step and do not refer to specific chemical species or mechanisms.

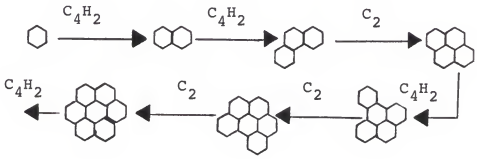

Another pathway for soot formation is given below for soot and PAH formation through direct aromatic condensation in which aromatic units remain intact. The constituent o-Terphenyl is at minimum equilibration concentration relative to both larger and smaller molecular intermediates in this polymerization pathway. Stein concluded that soot formation must occur through PAHs that represent the most favored thermodynamic path.

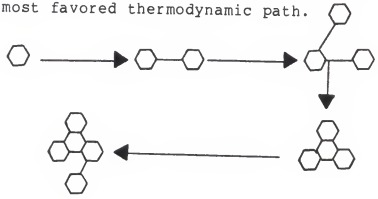

As a summary of the above discussion concerning neutral mechanisms leading to soot formation, one can conclude that each of these hypothetical mechanisms has been criticized in one or more of its intermediate steps. This demonstrates the lack of rigor in their concepts, primarily owing to the complexity of the subject.

Ionic Mechanisms

Introduction

It has long been recognized that flames conduct electricity and therefore contain ions. The lack of a unifying mechanism involving neutral and free-radical nucleation processes and the weaknesses encountered in the mechanisms proposed above have encouraged the consideration of an ionic mechanism as a possible process of soot nucleation in flames.

There are now improved mass spectrometric techniques that permit measurements of detailed ionic profiles in both fuel-lean and fuel-rich flames. Such techniques are allowing researchers to examine the ion chemistry involved in the formation and loss of ions in flames (Goodings et al., 1979a&b).

Calcote (1981) reviewed many of the proposed mechanisms of soot nucleation, both neutral and ionic, and presented a case favoring an ion--molecule scheme in which the ion $C_3H_3^+$ plays a leading role. This scheme is based on the $C_3H_3^+$ molecule's abundance and its characteristic

profile in a flame front. Before examining such an ion--molecule scheme and other possible routes leading to soot formation, we will present some cited experimental observations (Olson and Calcote, 1981a) that had provided a basis for a possible ionic mechanism. They are 1) a positive correlation is observed between the growth of large ions and the appearance of soot; 2) the concentration of large ions in diffusion flames and the onset of soot formation are both increased by electrophilic molecules; 3) the propensity of a fuel to soot is directly related to its ability to produce ions; 4) large concentrations of ions appear in pyrolysis experiments; 5) reactions of oxygen atoms with acetylene yield very rapid ionic polymerization; 6) concentration of the molecular ions peaks at the same location as the soot precursors; 7) the concentration of chemi-ions is estimated to be large enough to account for the concentration and rate of particles formed.

Wittig and Lester (1978) concluded from their experimental observations on the effects of electric field that positive ions appear to play a role in the nucleation of carbon particles; however, it is not clear whether it is the charge on the ion or its chemical nature that is important in initiating the formation of carbon particles.

Ionic Mechanisms

The overall process of soot formation from primary molecular species to soot aggregate is similar for mechanisms involving both neutral and ionic species. The

difference is that for ionic mechanisms, the nucleation sites, along with PAHs and virgin particles, are ionic in character.

The primary objection to an ionic mechanism is the small relative concentration of ions in flames as compared to hydrocarbon radicals (Michaud et al., 1981, Homann and Wagner, 1968). Figure 2-1 shows the concentration profiles of key neutral and ionic species as functions of distance above a burner (Calcote, 1981). Examination of the data shows effectively that concentrations of ions are orders of magnitude less than of polyacetylene or free radicals; however, the concentration of large positive ions exceeds that of soot particles, so it is clear that sufficient ions exist to serve as nuclei for particle growth (Wersborg et al., 1975). Also, it can be seen from this figure that the build-up and decay of relevant species seem to be consistent with a sequential ion-molecule reaction leading to a rapid build up of large ions (300-1000 amu range) and then to formation of soot.

Although many ionic mechanisms leading to soot formation have been postulated, there is still no complete agreement among workers for an ionic scheme describing the nucleation process. The controversy regarding any proposed ionic route can be attributed to the sparse experimental information available on how positive ions initiate the growth of soot nuclei. It has been generally accepted that

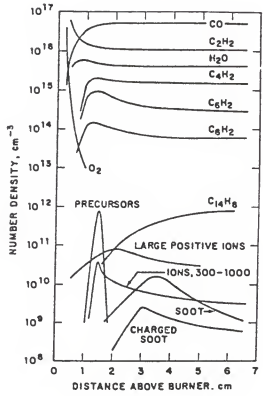

Figure 2-1. Number Densities of Various Species Found within Flames. Reprinted from the Article by H. Calcote (1981).

formation of primary ions occurs in a very thin, reactive zone (Bittner and Howard, 1981), via the chemi-ionization reaction first proposed by Calcote (1962):

$$CH + O \longrightarrow CHO^+ + e^- \quad (1)$$

or $$CH^* + C_2H_2 \longrightarrow C_3H_3^+ + e^- \quad (2)$$

Reaction (1) has been postulated to account for the large concentration of $C_3H_3^+$ observed in fuel-rich flames (Knewstubb and Sugden, 1959). However, this reaction has been discounted as a major contributor to the total ion density (Kinbara and Noda, 1971 & 1973, Miller, 1973; Peeters and Van Tiggelin, 1969). Extensive proton transfer reactions that neutralize CHO^+ follow rapidly so that this ion is never observed in large concentrations. Numerous flame ions obtained from secondary reactions have led investigators in flame chemistry to suggest various hypothetical reaction schemes in an attempt to explain the evolution of ion populations from the upstream region, through the reaction zone to the burnt gas region of a flame. Such a scheme includes

$$CHO^+ + H_2O \longrightarrow H_3O^+ + CO \quad (3)$$

$$CHO^+ + C_2H_2O \longrightarrow C_2H_3O^+ + CO \quad (4)$$

$$C_2H_3O^+ + C_2H_2 \longrightarrow C_3H_3^+ + CH_2O \quad (5)$$

$$CHO^+ + C_2H_2 \longrightarrow CO + C_2H_3^+ \quad (6)$$

$$CH_3^+ + C_2H_2 \longrightarrow C_3H_3^+ + H_2 \quad (7)$$

Reaction (3) leads to the formation of the dominant ion H_3O^+ observed to persist downstream of the reaction zone.

Reactions (4) and (5) were suggested by Olson and Calcote (1981a&b) to account for the large concentration of $C_3H_3^+$ in near stochiometric and lean flames. Reactions (6) and (7) have also been suggested by the same workers as a possible reaction route that does not require oxygenated species to account for the large concentration of $C_3H_3^+$ in rich flames (Olson and Calcote, 1981a&b).

Calcote (1981) has presented a case for an ion--molecule scheme in which $C_3H_3^+$ plays a leading role in the subseqent ion--molecule reactions in flames. This has been further elucidated by experiments of Olson and Calcote (1981b), who have employed a mass spectrometer to sample positive ions at different equivalent ratios in premixed flames. Their results show that $C_3H_3^+$ is the most abundant ion in fuel-rich acetylene and benzene flames. Further, as the flames are made richer, a drastic increase in large ion concentrations occurs at the expense of small ions (Figure 2-2).

Similar observations concerning the abundance and characteristic profile of $C_3H_3^+$ throughout the flame front have been reported by Michaud et al. (1981). Although they have recognized the importance of $C_3H_3^+$ for the subsequent ion chemistry in the burnt gas region, they have been reluctant to accept an ionic mechanism leading to soot formation.

Experiments have been conducted by Smith et al. (1982), and Eyler (1984) to show the effect of hydrocarbon ionic structure on reactivity. In order to compensate for

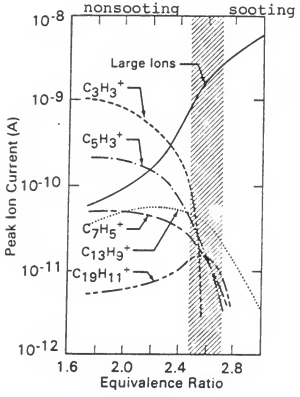

Figure 2-2. Effect of Equivalence Ratio on Peak Ion Currents for 2.0 KPa Acetylene-Oxygene Flames. The Shaded Area Indicates the Minimum Equivalence Ratio for Soot Formation: Reprinted from the article by Calcote (1981).

the lack of thermochemical data for isomeric hydrocarbon ions, two $C_3H_3^+$ structures (cyclic and linear isomer) have been investigated by Eyler (1983). Both have been made to undergo rapid reactions with a variety of unsaturated molecules, thus leading to higher molecular weight ions through condensation reactions.

$$C_3H_3^+ + \begin{cases} C_2H_2 \longrightarrow C_5H_5^+ \\ C_4H_2 \longrightarrow C_7H_5^+ \end{cases}$$

Vinckier et al. (1977), in their O-atom reaction studies in flow tubes, observed that CHO^+ is the dominant primary chemi-ion observed for real hydrocarbon flames, but other chemi-ions can be expected ($C_2H_3O^+$ has been observed in several flames). It has also been suggested by these authors that the secondary chemi-ion is obtained through the following proton transfer reaction:

$$CHO^+ + C_2H_2 \longrightarrow C_2H_3^+ + CO$$

$C_2H_3^+$ then polymerizes rapidly with acetylene to form $C_{2n}H_{2n+1}$ and $C_{2n}H_{2n-1}$.

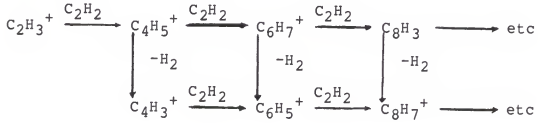

These early ionic polymerization are interpreted as the nucleation steps in soot formation in rich flames.

Brill and Eyler (1981) proposed a possible sequential ion--molecule polymerization if $C_2H_2^+$ ions were present in sooting flames:

$$C_2H_2^+ \xrightarrow{+\ C_2H_2} C_4H_2^+,\ C_4H_3^+ \xrightarrow{+\ C_2H_2} C_6H_4^+,\ C_6H_5^+ \longrightarrow$$

The rate constants for the condensation reactions above are smaller for each successive step. The next overall step in the nucleation process is the growth of larger hydrocarbons by further addition of the building block C_xH_y, to the primary intermediate ion produced above. The growth process occurs by rapid condensation. Condensation--elimination reactions are followed by a rapid rearrangement from linear to a more stable polynuclear structures (Stein, 1983). This is due to the characteristic of gaseous ions to rearrange to their most stable structure (Calcote, 1981)

Like the proposed neutral species mechanisms, the ionic mechanism also encounters some weaknessess in its formulation. The sequential ion--molecule mechanism of growth proposed by several of the workers above has been debated by Michaud et al. (1981). Because of the small concentration of ions in flames, they suggest that the source of large hydrocarbon ions can be explained as an equilibrium ion-molecule reaction between $C_3H_3^+$ and larger neutral species. Goodings et al. (1979b), in their interpretation of the ion chemistry in rich CH_y-C_2H_2-O flames, showed the relatively small importance of

condensation reactions when compared to proton transfer and, to a lesser extent, charge transfer throughout a flame in the chemical ionization of neutral species. Further, they have concluded, from their observations of hydrocarbon anions downstream of the reaction zone, that these anions could be formed by proton transfer from neutral hydrocarbon species which are resistant to destruction, by associative detachment with the H atom, i.e.,

$$C_nH_x^- \longrightarrow C_nH_x + e^-$$

Finally, the latter authors have suggested that the negative ions might explain the neutral chemistry in the early chemical stages leading to soot formation.

Soot Emission Models

Numerous attempts have been made to develop a comprehensive kinetic model for soot formation; however, models that estimate the rate of soot production in flames are very few. Although the hypotheses put forward by several workers (above) were sought to be interpretive of the chemical aspect of soot formation, the number of elementary chemical reactions associated with the process of formation of soot particles are excessively large for inclusion in a predictive model. Furthermore, in real combustion flames, emission of soot particles is controlled not only by chemical kinetics but also by heat transfer and fluid mechanics. The interaction between these processes makes modeling of soot emissions even more difficult.

Few cited models on soot formation and oxidation will be discussed in this section. The purpose of this discussion is not to validate or refute any of the proposed models, but rather to give some insight to the complex problem of modeling soot emissions.

The most comprehensive model for predicting the rate of formation of soot from gaseous hydrocarbons is the one proposed by Jensen (1974), who attempted to use detailed kinetic mechanisms to deal with all stages of soot formation. He suggested a model to describe the production of soot from a gaseous hydrocarbons in five steps: gas reactions producing radical fragments (fuel pyrolysis), nucleation, coagulation, growth, and oxidation. He considered fragments such as C_2, C_3, and C_2H as initial nuclei. Although the predictions made for a methane flame agreed with experiments, the utility of this model is limited because little information is available on the intermediate elementary reactions in the pre-particle chemistry.

Tesner et al. (1971) developed a simpler model which uses a global rather than a detailed approach to characterize soot formation. It is formulated in terms of equations that relate the rate of formation of active nuclei to the experimentally determined rate of formation of soot particles. In contrast with Jensen's model, Tesner's model does not specify the chemical nature of the

radical nuclei. The rate equations describing the formation of the radical nuclei and the soot particles are expressed as

$$\frac{dn}{dt} = n_o + (f-g) - g_o Nn$$

$$\frac{dN}{dt} = (a-bN)n$$

in which

n = concentration of active nuclei

n_o = spontaneous origination rate of the active nuclei

f-g = linear chain-branching coefficient

g_o = linear chain-breaking coefficient

N = concentration of soot particles

a and b are empirical kinetic coefficients

The value of a was determined analytically to be equal to the product of b and the maximum measured concentration of soot particles N_m at a corresponding time t_m. Subsequently, the values of the other coefficients (N, f-g, and b) were found using an iterative technique.

The rate of spontaneous formation of radical nuclei is evaluated by means of a rate equation:

$$n_o = AC \exp(-E/RT)$$

in which A is the frequency of oscillation of atoms along the bond being broken, E is the activation energy, and C is the concentration of fuel molecules.

Magnussen (1981) expanded such a two-step approach to the study of soot formation in turbulent flames to include the interaction between chemistry and turbulence. He assumes that chemical reactions are confined to regions consisting of fine structures, described as laminar sheets surrounding big eddies, generated by intense turbulent molecular mixing. The reaction volume and the mass transfer rate between these fine structures and the surrounding fluid have to be known in order to treat the chemical reactions within this space.

A modified version of this model was devised by Galant et al. (1984). The calculations of soot concentration calculations reported by Magnussen and Galant using both laboratory and large scale diffusion flame show satisfactory agreement with their corresponding experimental results.

A model based on a so-called "quasi-global" scheme was introduced by Edelman and Fortune (1969). This model is a compromise between the complex detailed mechanism and the simplistic but less informative global reaction scheme.

The quasi-global kinetic mechanism is an extension of the notion of a single-step overall reaction to a set of important reactions. This scheme characterizes the partial oxidation of large hydrocarbon molecules by sub-global steps coupled with a set of finite, reversible reactions for which sufficient information exists, and treats soot formation similarly to the formation of other species.

Edelman et al. (1979) developed an expression for the rate of soot formation in a jet-stirred reactor.

$$R_S = A\ T^a\ [HC]^b\ [O_2]^c \exp(-E/RT)$$

where a, b, and c are dimensionless constants, E is the activation energy, and [HC] is the concentration of unburned hydrocarbon.

The rate of soot formation and other global rates are evaluated by direct comparison of predictions with experimental data. The quasi-global mechanism predicts the unburned hydrocarbon and oxygen concentrations and temperature required in the global reaction for soot formation. Net soot production can be estimated using the following conservation equation (Farmer et al. 1981):

$$\frac{\dot{m}}{\rho V} = C_s - C_{s,0} = A_t R_{ox} - R_f$$

where $\dot{m}$, ρ, V, C_s, $C_{s,0}$, and A_t are total mass flow rate, exhaust gas density, reactor volume, outlet and inlet soot concentrations, and the total surface area available for oxidation, respectively. The reaction rates for the soot formation and oxidation steps are R_f and R_{ox}, respectively.

A quasi-global kinetic model for toluene and iso-octane developed by Edelman et al. (1983) showed an acceptable fit with experimental data. A set of Exxon jet-stirred combustor experiments was the primary source of data to establish the model.

Khan and Greeves (1974) presented a semi-empirical Arrhenius type equation for the local rate of soot formation in diesel engines. The phenomenological aspect of soot formation was not suggested in this model. Furthermore this model is based on experimental values of local temperature, unburned hydrocarbon concentration, and the local equivalence ratio which can change from one experiment to another.

The oxidation step is very important in understanding soot particle emissions. The multitude of potential oxidants (O, O_2, OH, CO) that can participate in the oxidation step, depending upon conditions, prevents complete agreement on a universal formula that will best predict the oxidation rate of soot particles in flames.

Radcliffe and Appleton (1971) suggested that the surface mechanisms for oxidation of pyrolytic graphite and of soot are similar. A semi-empirical expression, originally proposed by Nagle and Strickland-Constable (1962) for oxidation of graphite, was used by different workers (Chul and Appleton, 1973; Edelman et al., 1979; Appleton, 1973) to predict the rates of oxidation of soot. The rate of oxidation of soot per unit area of soot surface is formulated as follows:

$$R_{ox} = 12 \frac{k_A P_{o2}}{1+k_z P_{o2}} \times k_B P_{o2} \quad (1-X)$$

where

$$x = 1 + \left(\frac{k_t}{k_B P_{O2}}\right)^{-1}$$

This rate equation is based on the theoretical model of the surface oxidation rate mechanism originally proposed by Blyholder et al., (1958). The values of k_a, k_b, k_t, and k_z were obtained by Nagle and Strickland-Constable (1962) to fit their measurements.

$k_a = 20 \exp(-30/T)$ g cm^{-1} sec^{-1} atm^{-1}

$k_b = 4.46 \exp(-7{,}460/T)$ g cm^{-2} sec^{-1} atm^{-1}

$k_t = 1.51\ 10^5 \exp(-48{,}800/T)$ g cm^{-2} sec^{-1} atm^{-1}

$k_z = 21.3 \exp(2{,}060/T)$ atm^{-1}

Lee et al. (1962) measured rates of oxidation of soot in a laminar hydrocarbon flame. Soot particles and samples of combustion gases as well as temperature were measured at different cross-sections of a hollow soot column. A semi-empirical rate equation that is dependent on the temperature and partial pressure of oxygen was suggested:

$$R_{ox} = 1.085\ 10^4\ P_{O2}\ T^{-1/2} \exp(-E/RT)$$

The first-order dependence of rate upon the partial pressure of oxygen was criticized by Appleton (1973). He concluded from his experimental results in a shock tube that at fixed temperature and low oxygen partial pressure, the surface oxidation rate is first order in partial pressure of oxygene and approaches zero order at high pressures.

Neoh et al. (1981) investigated the potential oxidants of soot in both fuel-rich and fuel-lean flames. Their experiments showed OH contribution to be more important than O_2 in the oxidation of soot in atmospheric flames between 1575 and 1865K. Comparison of their experimental rate to the rate predicted from the Nagle--Strickland-Constable formula agreed for lean flames; however, discrepancies between the two rates became larger as the flames were made richer in fuel. According to Neoh and coworkers, the neglect of the contribution of OH in the predictive formula of Nagle and Strickland-Constable was the cause of the observed discrepancies.

Experimental Observations

To interpret soot-related measurements of chemical species and concentrations of particles in flames, it is necessary to determine the parameters that affect the processes governing soot formation and oxidation and to attempt to explain the drastic changes in the evolution of the soot field that occur between fuel-lean and sooting flames.

It has been recognized that the equivalence ratio correlates the tendency of fuel to soot (Street and Thomas, 1955); however, this parameter is based on a reaction scheme where only CO_2 and H_2O are produced in oxygen rich-flames. This is not the case at the sooting limit where carbon monoxide is in excess of CO_2. Takahashi and Glassman (1982) proposed a more-general formalization for

expressing the tendency of fuel to soot. It is based on a stoichiometric reaction in which the carbon is converted to carbon monoxide and the hydrogen is converted to water. The proposed variable for indicating the tendency of hydrocarbons to soot in premixed flames is the ratio (C + H/2)/O, where the numerator expresses the stoichiometric oxygen requirement on this new basis and the denominator is the actual experimental value of oxygen at the onset of sooting; however, in diffusion flames soot, particles are formed in the fuel side of the flames (Kent et al. 1981) where the concentration of oxygen is insignificant. Hence, the equivalence ratio is not an appropriate parameter that can correlate the sooting tendency of a fuel in a diffusion flames. Next, the recent developments in the study of soot formation in shock tubes and flames will be reviewed.

Pyrolysis of Fuel

Shock tube techniques have been very useful in the study of soot formation. They allow one to produce time invariant, controlled conditions of temperature and pressure similar to those in real flames. This permits examination of the temporal behavior of reactant and product concentration at constant temperature and pressure. Selected fuels have been investigated by pyrolysis behind incident or reflected shock waves (Graham, 1977; Frenklach et al., 1982;) and are reviewed briefly here.

Influence of the induction time

Initial formation of carbon particles occurs after an induction period that is characterized as a function of temperature, pressure, and molar concentration of hydrocarbons. This parameter, although subject to criticism related to the credibility of its measurement, can be useful when relating soot formation to residence times in particular regions of combustion chambers.

Influence of pressure

Frenklach et al. (1983 a&b) observed that for homogeneous hydrocarbon/air mixtures at low pressure ($P < .1$ bar), the maximum measured soot yield is shifted to higher temperatures; however, at higher pressures (1 to 10 bars) an increase in pressure increases soot yield slightly. This dependence of soot yield on pressure during soot formation in pyrolysis of aromatic hydrocarbons was interpreted by Frenklach et al. (1983a) as follows: A decrease in pressure slows down decomposition reactions and at constant soot yields production, an increase in temperature is needed to compensate for the decrease in total pressure. This explains the shift of a soot-bell maximum to higher temperature.

Influence of temperature

Several experimental observations (Frenklash et al., 1982, 1983b; Wang et al., 1981) have shown a bell shaped dependence of soot yield on temperature in the pyrolysis of

a variety of hydrocarbons. Frenklach et al. (1983a) concluded from an extended analysis of xylene pyrolysis that the position of the maximum in soot yield is not universal but rather dependent on observation time, pressure and extinction mode. Rawlins et al. (1982) observed no soot in toluene pyrolysis below 1500K or above 2500K, and a maximum soot yield of 30-50% of the initial fuel carbon near 2000K.

Premixed Flames

Mass spectrometric and optical techniques have been used extensively in premixed flames to identify hydrocarbon species (stable products, radicals, and ions) which can serve as detailed probes of combustion chemistry. The soot formation chemistry in premixed flames is not complicated by the diffusion processes that are characteristic to diffusion flames.

Prado et al. (1981) identified two regimes for soot particles growth in premixed flames. For soot volume fractions less than 10^{-7}, particle growth occurs by coalescent coagulation. At larger soot volume fractions, chain-forming collisions occur simultaneously with surface growth. Laser light scattering and absorption techniques have been used to characterize particle size and number density profiles in premixed flames (D´Alessio et al., 1977; Haynes et al., 1981). It has been observed that the number of particles near the reaction zone is large (10^{11}-10^{12} cm^{-3}) and the corresponding "soot" particles are

small (the smallest particle diameter detectable by laser light scattering methods is about 2.0 nm). Smyth and Mallard (1981), using laser induced ionization in premixed flames at the sooting limit, measured particle masses in the range 2300-6100 daltons, having diameters of 1.6-2.2 nm. This is in the range of the lower limit of particle diameters (1.5 nm) that can be detected by electron-microscopic techniques.

Beyond the soot limit, the yield of soot in premixed systems increases very rapidly with C/O ratio. This is the result of increased nucleation sites for elementary soot particles to form as the carbon--oxygen ratio increases (Wagner, 1981).

The effect of metal additives on soot formation in premixed flames was recently investigated by Haynes et al. (1981). This work investigated the impact of alkalimetals and alkalineearths injected into the post reaction zone of premixed flames. They concluded that these additives do not reduce soot as expected by many workers, but rather, they increase the number of smaller, charged soot particles that subsequently resist coagulation by Coulombic repulsion.

Glassman (1979) argued that temperature is a very significant parameter associated with processes of soot formation and oxidation. He supported Millikan´s concept (1962) that under premixed conditions the rate of soot formation is controlled by the competitive process between

the rates of pyrolysis of fuel and oxidation of soot precursors. Because the rate of fuel pyrolysis is less sensitive to an increase in flame temperature than the rate of soot oxidation, raising the temperatures lowers the tendency to soot.

Harris (1982) examined the processes leading to surface growth in premixed C_2H_4/air and $C_2H_4/Ar/O_2$ flames. He concluded that acetylene in combustion products is the source of mass for most mature soot particles. Furthermore, this author determined that C_2H_2 occurrence is a first-order with respect to soot growth.

Calcote and Manos (1983) reviewed the literature and investigated the results of soot measurements in both premixed and diffusion flames. They defined a numerical index called the "Threshold Soot Index" (TSI), which can be used quantitatively to compare and analyze sooting flame data. This soot index ranks the fuels from 0 to 100 (0 = least sooty).

Diffusion Flames

Diffusion flames are very important in simulating phenomena occurring in most combustion devices. Unlike premixed flames or the homogeneous mixture used in shock tube research, the diffusion flame is mixing controlled.

The height at which a diffusion flame starts to smoke and the corresponding luminosity of the flame are considered a measure of the tendency of a fuel to form carbon. Velocity has a direct effect on the height and the

brighthness of the flame. As the velocity of the fuel jet increases, both the flame height and the luminosity increase. Finally, a limit is reached where the flame begins to emit soot. Unfortunately, spatially resolved mapping of soot distribution in diffusion flames is difficult owing to steep concentration and temperature gradients, and to the inhomogeneity of the mixture in such flames (Kent et al., 1981). As particles travel through the flame field, they pass through regions where conditions vary widely. Concentration, Size, temperature, and flow velocity of soot particles are not only dependent on the height in the flame, but also on radial position owing to non-axial flow velocity and particle diffusion.

The development of laser light-scattering measurements and other non-intrusive optical techniques has enhanced the spatial resolution of particle mapping throughout the flame. In their study of soot particle formation and growth in a co-annular diffusion flame, Santoro et al. (1983) observed that the flame can be divided into two regions. The first is characterized as a region of growth in which soot formation dominates. The second is characterized as a region dominated by oxidation processes. Rates of soot production have been found to be higher near the base of the flame where the temperature range is 1200-1400 ^{o}C; The production rate decreases with the distance from the flame (Kent et al., 1981). The soot formed near the base of the flame is transported upward by convection

and radially by both diffusion and convection (Santoro et al., 1983; Kent et al., 1981). Kent et al. (1981) observed that small flames have higher initial soot volume fractions and particle growth, but larger flames have a greater soot volume fraction higher up in the flame because of their longer relative residence times.

Glassman (1979) determined that in diffusion flames, oxidative rates do not increase as fast as pyrolysis rates with respect to temperature. Thus, the higher the temperature, the greater tendency to soot. Wey et al. (1982) confirmed the latter result in their studies. These researchers observed that higher temperatures also lead to large soot particles and agglomerates that are difficult to burnout downstream of the flame.

Turbulent Diffusion Flames

The unsteady nature of turbulent diffusion flames results in a nonhomogeneous distribution of fuel in air. Conceptually, this can be represented as pockets or eddies of gas with different fuel-air ratios (Prado et al., 1977) distributed throughout the flame region. Soot is assumed to be formed and contained in these eddies, which are separated by regions containing little or no soot (Magnussen et al., 1979). These inhomogeneities are attributed to the interaction between turbulence and chemical reactions.

It has been suggested by Becker and Yamazaki (1977) that soot formation and burnout in diffusion flames is essentially mixing controlled. The principal aerodynamic parameter that controls soot formation is the Richardson ratio (Ri), which relates the effect of buoyancy to momentum forces. Becker and Yamazaki discounted the Reynold's number (Re), as an important parameter, since the action of buoyancy, even at low Reynolds number, increases the downstream momentum flux such that virtually all flames are fully turbulent; however, Magnussen (1981), in his eddy-like intermittency model, observed that for a given nozzle diameter, variations of the Reynolds number significantly affect the amount of soot formed.

Nishida and Mukohara (1982) demonstrated that when the inlet air temperature is raised from 50 to 500^{o}C, the gas temperature on the flame axis increases by 100-300^{o}C. The concentration of soot and hydrocarbons was shown to be greater and the decay of soot concentration more rapid in the higher temperature flames.

CHAPTER III
EXPERIMENTAL METHODS

Characterization of molecular species and particulates as they exist in a combustion environment is necessary to improve the understanding of the processes that lead to their formation and destruction in that environment. Such characterization requires a diagnostic technique that does not interfere with the measured properties of interest and that can provide adequate spatial and temporal resolution of the data.

Physical sampling probes have been used to observe changes in particle size and population density in the combustion environment; however, they are inherently slow and intrusive, and they require tedious sampling procedures and analysis. The emergence of optical techniques has enhanced the study of molecular species and particulates in combustion. These techniques provide rapid data acquisition and resolution while causing only minimal disturbance to the actual phenomena. This research effort stressed the use of an optical technique to measure size and population density of soot particles (Integrated Particle Sizing System (IPSS)). Physical probes provided necessary support for validation of the IPSS, and they were

also used in this work to complement data collection in such areas as temperature measurement and gas sampling, for which optical instruments were not available.

Modular Burner

The burner used for the current study is a non-premixed axisymmetric bluff-body type combustor exhausting into free air. Studies on this type of combustors were initiated by the Air Force Wright Aeronautical Laboratories/Aeropropulsion Laboratory (Roquemore et al., 1983). The simple configuration of such combustors provides easy optical access for measurement purposes and good flame stabilization.

The bluff-body burner (Figure 3-1) consists of a central fuel pipe surrounded by an annular region through which air flows. The fuel passes through the central pipe and exits through a 1.37-mm diameter nozzle located in the center of a 5.72-cm OD aluminum centerbody. Compressed air (relatively free of contamination by particles, water, or oil droplets) enters the plenum chamber surrounding the central fuel pipe, passes through flow straighteners, and exhausts at the burner exit plane, where the mixing process occurs. The fuel, nitrogen dilution, and air flow rates through the system are monitored through an easily accessible control board (Figure 3-2).

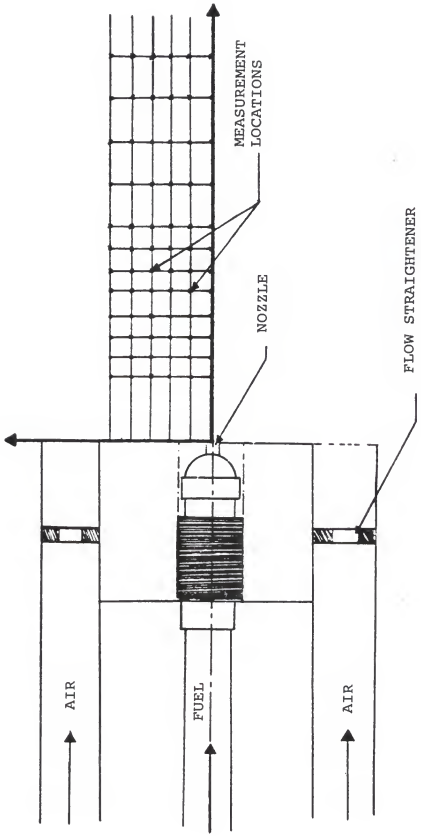

Figure 3-1. Schematic of the Bluff Body Burner

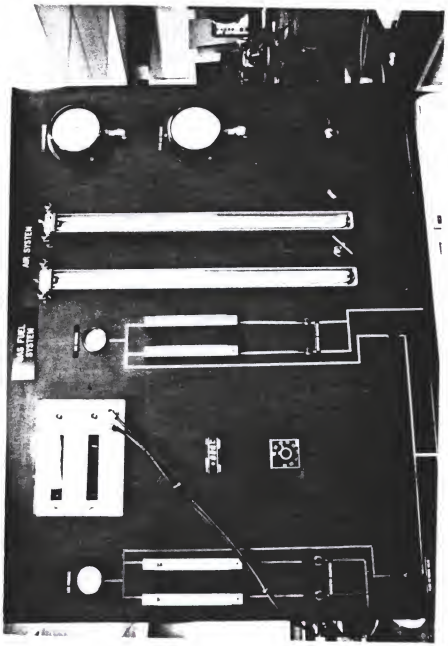

Figure 3-2. Control Board

Physical Sampling

Extractive Probe and Sampling System

Sample extractions at a point in a flame or in the exhaust system were performed with an extractive probe (Figure 3-3) provided by the University of California Irvine Combustion Laboratory. This sample probe was designed to collect soot samples and combustion gases for chemical and physical analysis. The design considerations of the extractive probe and sampling system were carefully reviewed (Hack et al., 1981) and will not be presented in this report; however, a succinct description of the probe and the sampling system is presented below.

The probe consisted of a sample transport tube surrounded by an annular jacket through which cooling water circulated. Stainless steel (316) was used for all surfaces exposed to the sample or the combustion environment. The outside diameter of the probe was 0.375 in (0.953 cm). and the sample tube diameter was 0.12 in (0.305 cm). The overall length of the probe was 25 in (63.5 cm) (from the tip to the mounting plate) with a curvature of 20 in (50.8 cm).

Cooling water was carried through seven 0.043-in (0.109 cm) ID tubes inside the annulus to the probe tip and returned through the remaining annular space. The cooling water was circulated to maintain the probe temperature below the design limit of stainless steel.

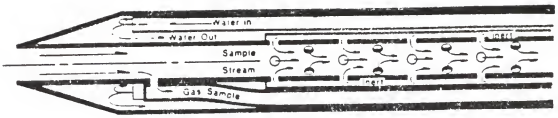

Figure 3-3. Extractive Probe

Nitrogen was injected through thirty-two 0.031-in (0.079 cm). diameter holes organized into eight groups of four holes. Dilution with nitrogen was necessary to minimize particulate deposition on the walls of the sampling line. A separate port in the mounting plate was included for extracting gas samples.

The sampling system consisted of a filtration bank in which Nuclepore filters (0.47 mm OD) and 0.2 micrometer pore size were used, a dry test meter (DTM), four rotometers for volume determination, and a vacuum pump for isokinetic sampling.

Direct particle collection.

The face of the burner and a filter (Figure 3-4) located about six feet (183 cm) downstream in the exhaust system were chosen as sites to collect soot particles for chemical analysis. The former was chosen because of the relatively low temperature existing at the face of the burner (this cold surface allowed trapping of stable products that could be related directly to the intermediate hydrocarbons that form soot particles). The latter site was chosen to determine the chemical composition of components that survived the oxidation process and to determine their toxicity in relation to the environment.

Temperature Probe

Temperature measurements in sooting flames are difficult because soot deposits on a thermocouple causes an

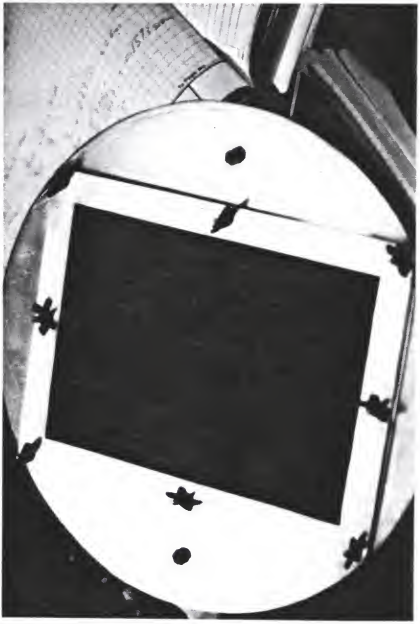

Figure 3-4. Soot Particle Filter.

increase in conductive and radiative losses; however, such measurements do provide valuable information that can be used with soot particle and velocity measurements to complement the study of soot evolution in flames.

Temperature profiles were obtained with Pt/Pt-10% Rh fine wire thermocouples that were made of 0.006-in (0.015 cm) diameter coated wires (platinum--rhodium as a sheat material and magnesia for insulation) with a welded junction of nearly the same diameter.

Integrated Particle Sizing System

This study involves the use of an Integrated Particle Sizing System (IPSS) capable of providing nonintrusive, in-situ, real-time measurements of particulate size and population density in flames. The technique is based on the theory for scattering of a plane, linearly-polarized light wave by a single, homogeneous, isotropic sphere of arbitrary size and refractive index, first formulated by Mie in 1908 (Kerker, 1969). Since the technique is based on light scattering from spherical particles, Mie theory is discussed first, followed by the system description.

Mie theory.

Mie´s theory is based on a formal solution to Maxwell´s equations, with appropriate boundary conditions applied to the scattering of light by a homogeneous sphere of arbitrary size and refractive index. The mathematics and the corresponding assumptions that led to the

formulation of the solution are given elsewhere (Van de Hulst, 1981; Kerker, 1969) and only a few results relating the solution to the problem of interest are repeated here.

The solution takes the form of an infinite series of Bessel and Legendre polynomials. The radiant flux $\underline{P}$ scattered by a particle can be expressed as

$$\underline{P} = \frac{I_o \lambda^2}{4\pi^2} \int_{\theta_1}^{\theta_2} \int_{\phi_1}^{\phi_2} i_1(\chi,m,\theta)\sin^2\phi + i_2(\chi,m,\theta)\cos^2 \sin\theta d\theta d\phi$$

where I_o is the incident intensity, λ is the wavelength of the incident radiation, r is the distance from the scatterer, m is the complex index of refraction, θ is the scattering angle, χ = is the size parameter, and ϕ is the angle between the scattering plane and the plane of polarization of the incident radiation. The Mie scattering functions for light polarized perpendicular and parallel to the scattering planes are i_1 and i_2, respectively. These functions are related to the amplitude functions as

$$i_1(\lambda,m,\theta) = S_1(\lambda,m,\theta)$$

and

$$i_2(\lambda,m,\theta) = S_2(\lambda,m,\theta)$$

Also it is customary to define the partial scattering cross-section C as the power of light divided by the the incident intensity (Sterling,1986) as

$$C = P/I_o$$

The Integrated Particle Sizing System uses a ratioing technique for particle size determination. The intensity ratio of the power of the radiation scattered by a particle and collected in the forward direction by lenses located at two different angles is

$$\frac{P\ (\theta_1)}{P\ (\theta_2)} = \frac{C\ (\theta_1)}{C\ (\theta_2)}$$

where is the large angle and is the small angle formed by the lens axes with the axis of the incident beam. The incident laser intensity cancels out, eliminating the problems associated with the Gaussian intensity distribution of the laser beam.

The intensity ratioing technique requires the determination of the Mie intensity functions i_1 and i_2, which can be generated by computer codes developed by a number of workers in this field (Dave, 1968). The input parameters are the size parameter ($\pi D/\lambda$), the wavelength of the incident radiation, the scattering angle, the refractive index of the surrounding media, and the complex refractive index of the sphere. A plot of the intensity ratio versus particle size for scattering at 20^o and 60^o is presented in Figure 3-5. The computation of

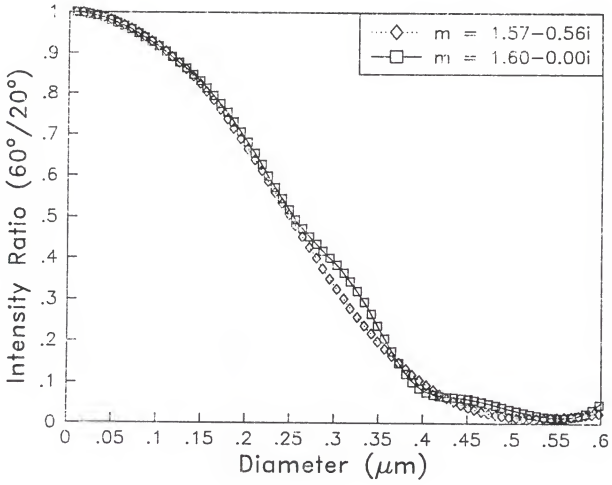

Figure 3-5. Intensity Ratio vs. Particle Size

intensity ratio versus particle size was carried out by Sterling (1986). The particle refractive indexes were for latex (m = 1.60) and soot (m = 1.57 - 0.56i).

System description

The Integrated Particle Sizing System includes 4 techniques for in-situ measurements of particle size, droplet size, and particle velocity. These techniques are (1) large-angle intensity ratioing, applicable to particles 0.08 to 0.6 μm in diameter; (2) small angle intensity ratioing, applicable to particles 0.3 to 3.0 μm in diameter; (3) particle sizing interferometry, applicable to particles 2.5 to 45 μm in diameter; (4) droplet sizing interferometry, which is applicable to droplets 2.5 to 140 μm in diameter. Because the focus of this work is characterization of submicrometer-sized soot particles, the large angle intensity ratioing technique was adopted for particle size and number density measurements.

The concept of the large-angle intensity ratioing technique is to collect the forward-scattered light from individual particles as each crosses the probe volume at two off-axis angles. This instrument was used to deduce their respective sizes from the ratios of the collected intensities. The relationship between particle size and intensity ratio is obtained from the solution of Maxwell´s equations (Kerker, 1969) describing the scattering of electromagnetic waves as derived by Mie for spherical particles of arbitrary size and

refractive index. The input parameters for this technique are the collection angle pair and index of refraction of the particles. The angle pair determines the particle size range to be measured.

Random stray signals associated with multiple scattering can overwhelm the scattering signals from the particles to be measured; however, this instrument can also be used as an optical counter if single-particle scattering is dominant over multiple-particle scattering. Single particle scattering requires that the laser light scatter from a single particle passing through the probe volume and propagate directly to the detectors without interfering with any signals from other particles that may be present in the particle cloud surrounding the probe volume. Single particle scattering can be promoted by providing a small probe volume at the test section, which, when combined with a high signal-to-noise ratio and fast data resolution, can enhance the performance of the system as a particle counter.

A schematic diagram of the measurement system is given in Figure 3-6. The incident radiation is supplied by a 2-W Argon Ion Laser operating in the multiline mode. The 488 nm line used for intensity ratioing is separated from the other lines by a dispersion prism. The beam is aligned by a series of mirrors, expanded by a variable beam expander, and linearly polarized in the direction vertical to the plane of scatter by a dichroic mirror. The

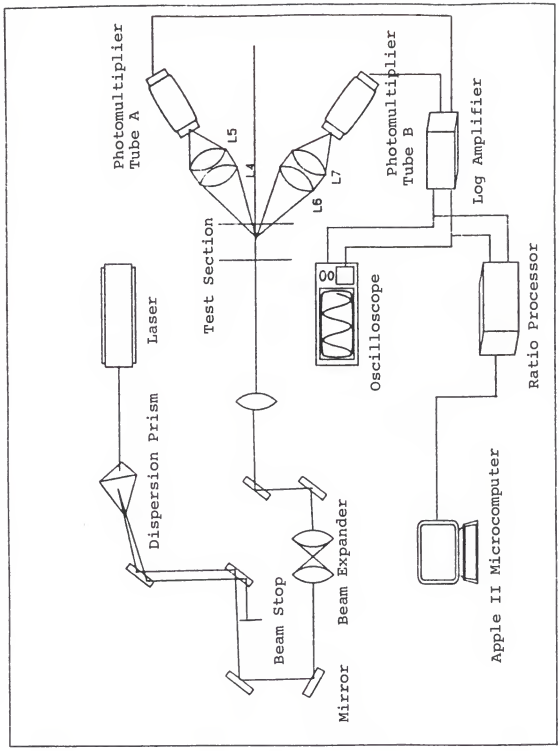

Figure 3-6. Schematic of the Integrated Particle Sizing System.

beam is focused by an 300-mm focal length lens to produce a waist that, in conjunction with the collecting optics, defines the sample probe volume of the instrument.

The light scattered by a particle passing through the probe volume is collected by two pairs of identical 300-mm focal length, f/4 lenses in the horizontal plane of the beam. The two pairs of lenses are contained in two cylindrical enclosures located at two angles off-axis of the incident beam. The angle pair ($60^{o}/20^{o}$) was used in this study to yield measurements of particle size in the range 0.08 to 0.39 μm. The focus of the first lens coincides with the sample point of the instrument. The first lens of each receiving system collects the scattered light and collimates it. The second lens focuses the beam upon a pinhole in front of a photomultiplier tube.

The detectors are RCA 8575 photomultiplier tubes (PMTs) powered by a high-voltage power supply (Bertran Associate, model PMT-20A/N (option 3)). These PMTs utilize a photosensitive cathode and a number of dynodes to convert the scattered light into current. The relationship between the collected light impinging upon the PMTs and the corresponding output current can be expressed as

$$i = c(F)(10^{kE})$$

where F is the radiant flux striking the cathode, E is the voltage supplied to the PMT, and c and k are constants specific to the PMT; F is equal to the power of the

scattered light, P, passing through the pinhole aperture divided by the sensitive area of the cathode.

Each PMT is equipped with a band pass filter with a bandwidth at half maximum of 2 nm and a transmitance of 20% at 488-nm. These filters discriminate against the background signals generated by stray light or luminous light from flames.

A dual logarithmic amplifier from Spectron Development Laboratories (SDL), Model LA-1000, used to convert the current pulses from the PMTs into positive voltages pulses, is scaled to a maximum output of 10 V for an input current of -1 mA. For pulse widths not less than 10 μs, the amplifier is rated for current amplitudes as small as 1 nA; for pulse widths as small as 2 μs, it is rated for amplitudes as small as 1 μA. The output of the log amplifier can be expressed as

$$V = 2 \log(i/i_o)$$

The output pulse voltages from the logarithmic amplifier are sent to a ratio processor (SDL, RP-1001). These signals are first buffered and peak detected. The dc level outputs from the peak detectors are fed to an analogue subtractor circuit which mechanically divides the signals at the large angle (A) by the respective signals at the small angle (B). The subtractor output is amplified to 0 to 10 volts and then converted into an 8-bit binary number by an analogue--digital converter. An output of 10 volts corresponds to a ratio (A/B) of 0.1 and 0 volts corresponds to a ratio of 1.0.

The ratio processor uses the seven most significant bits of the data word for data acquisition; the 8th bit in the data word is used as a status bit to indicate whether the current data word is valid or invalid. A zero level indicates a valid data word. This is determined by it meeting three conditions:

a. The B input signal level must be less than 10 volts.

b. The A input signal must be less than the input signal B and greater than a minimum level of 4 volts for high speed operation or 2 volts for low speed operation.

c. The width of the A input signal pulse must be greater than 2 μs for high speed operation or 10 μs for low-speed operation.

The digitized signals are then transferred to a microcomputer for data analysis. A histogram generator software package resolves the data output into 62 bins, of which each corresponds to a discrete size range. Typical output data of this technique are shown in Figure 3-7.

Aerosol-Generating System

Spherical latex particles of known size were used to evaluate the performance of the optical system both as a particle sizer and as a particle counter. These particles, which were supplied in mixtures in water and surfactant, were 0.5% and 10% solid by weight. They have a density of 1.05 g/ml and a refractive index of 1.57 at 488 nm.

Samples were prepared by diluting a highly concentrated particle suspension in de-ionized water or alcohol. The resulting suspension was passed through a

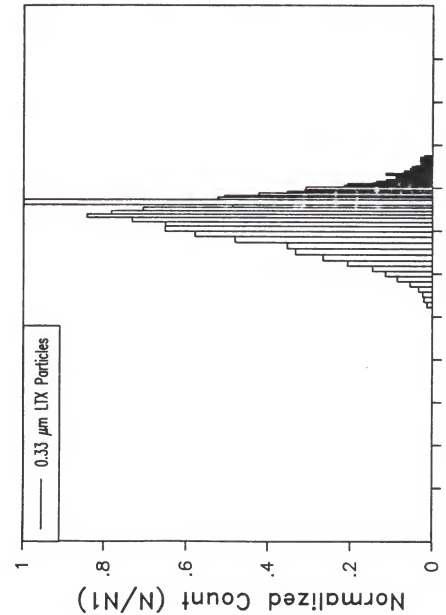

Figure 3-7. Typical Optical Data Output.

constant output atomizer to form droplets. A schematic diagram of the aerosol generation system is shown in Figure 3-8. Clean, dry air was supplied to the atomizer through a 0.343-mm diameter orifice to form a high velocity jet. The suspension was drawn by the jet to the atomizer, where large droplets were removed by impaction on the walls of the atomizer assembly. Excess liquid was removed continuously to a waste container.

A syringe pump (model 975, Harvard Apparatus Co.) was used to provide a regulated hydrosol flow rate to the atomizer. The pump has a synchronous motor and is capable of providing stable constant flow rates. The pump includes a 30-position gear box that allows the liquid flow rate to be varied from 0.027 to 46 cm^3/min when using a 50 cm^3 standard syringe.

The wet aerosol coming out of the atomizer was passed through an evaporation/condensation aerosol conditioner (TSI model 3072) to improve its monodispersity. A diffusion drier (TSI model 3062) was used to dry the aerosol; the aerosol was then injected through a nozzle centered just below the optical probe volume for measurements.

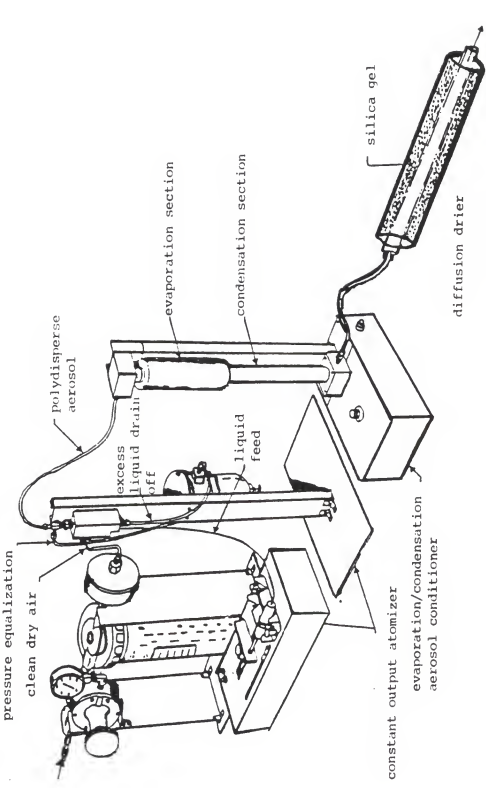

Figure 3-8. Aerosol Generation System.

CHAPTER IV
EVALUATION OF THE OPTICAL SYSTEM

A detailed analysis of the Integrated Particle Sizing System (IPSS) to evaluate its overall accuracy in measuring sizes and number densities of particles and its adaptability to different testing environments (reacting and non-reacting flows) is a necessary prerequisite for interpretation of empirical data for particulate characterization in combustion systems. The performance characteristic of the optical system is a strong function of the state and nature of the particle delivered to the probe volume as well as of the medium surrounding it.

The IPSS measures the rate at which particles pass through the sampling space defined by the intersection at the waist of the incident laser beam and the collecting optics of the system; however, the effective sampling volume can be affected by the intensity variation in the sample space (Figure 4-1) and the scattering characteristics of the particle to be measured. Therefore some refinement of the measured data for the IPSS can be realized, through probe volume corrections that would take into account both of these effects.

Experiments were performed to test and evaluate the optical system performance as a particle sizer as well as a particle counter in both cold (dispersion of latex

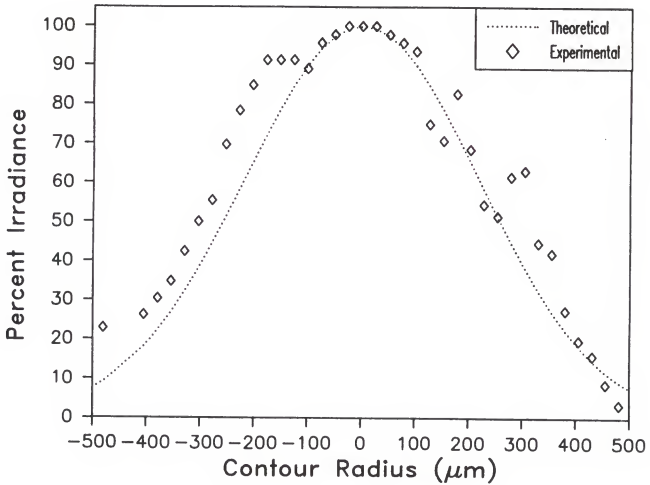

Figure 4-1. Laser Beam Intensity Distribution.

hot (combustion) media. The results of these experiments are presented next.

Cold Flow

Latex particles of known size were used to validate the system's performance as a particle sizing-instrument. These particles were diluted in liquid methanol to avoid scattering introduced by water droplets. Figure 4-2 shows the measured count mean diameter versus the nominal diameter of the particles. The measured diameters of the particles agree well with the corresponding sizes specified by the manufacturer.

The system's performance as a particle counter, in the limits of the measured size range, was investigated by measuring the particle count rates from suspensions with different latex particle concentrations; however, the flux rate at which particles pass through the probe volume was found to be dependent both on the particle concentration of the suspension and on the flow rate through the atomizer. Therefore, in order to verify the reliability of the system as a particle counter, the operating conditions of the atomizer had to be determined.

The characteristic operating conditions of the atomizer assembly were investigated using two suspensions with particle concentrations (Cl) and (Cl)/2; (Cl) was the reference particle concentration. The flow rate of the particle suspension was maintained at a known level with a

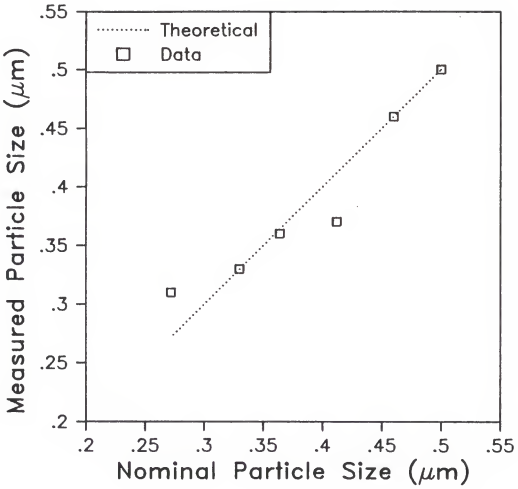

Figure 4-2. Measured Diameter Versus Nominal Diameter (μm)

syringe pump. The particle count rates versus flow rates for the two suspensions tested are presented in Figure 4-3. The results are consistent with expectations only at the lowest particle suspension flow rates. The effect of suspension concentration on the atomizer output decreased when the suspension flow rate was increased. The atomizer output became independent of the concentration of the suspension concentration when the flow rate was set above 8.6 cm^3/min.

One might speculate that a suspension having a high concentration of particles produced large droplets whose greater inertia caused their impaction on the walls of the atomizer resulting in a decrease of its output. In order to establish the particle concentration as the main variable controlling the atomizer output, the impaction of the droplets was reduced to a minimum by using low suspension flow rates.

The measured size distribution of the latex particles was found to be independent of the suspension concentration. Figures 4-4a and 4-4b show the normalized size distribution histograms for a suspension of 0.412-μm latex particle at concentration (Cl) and (Cl)/2, respectively. Virtually no shift in size distribution is observed.

The measured particle count rates for four suspensions with particle concentrations of (Cl), (Cl)/2, (Cl)/4, and (Cl)/8 are presented in Figure 3-5 for particle solution

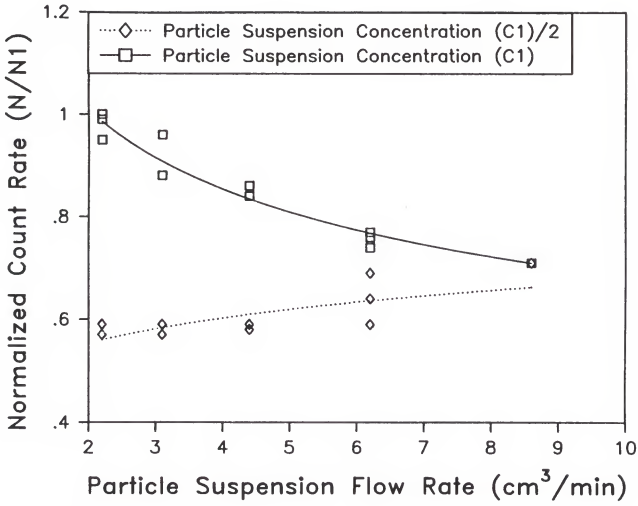

Figure 4-3. Particle Count Rate vs. Particle Suspension Volumetric Flow Rate.

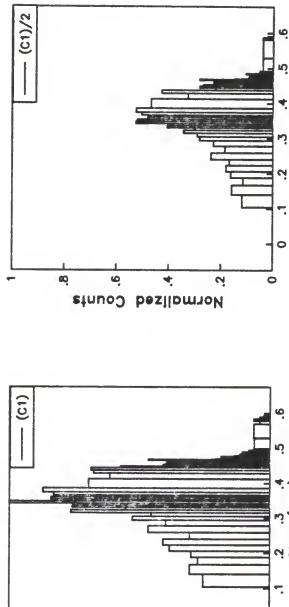

Figure 4-4a & b. Normalized Particle Count Rate vs. Particle Size.

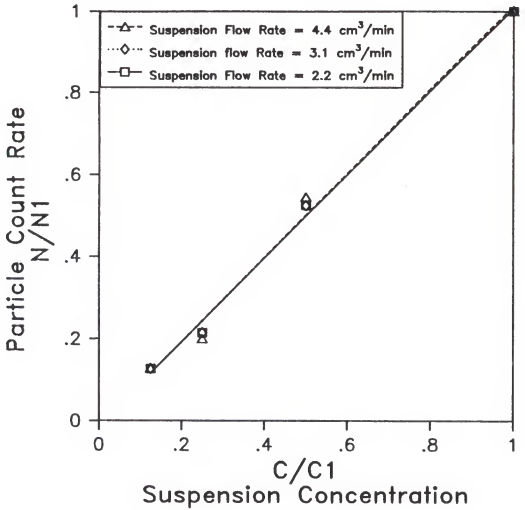

Figure 4-5. Particle Count Rate vs. Particle Suspension Flow Rate (Normalized)

flow rates of 2.2, 3.1, and 4.4 cm^3/min. For each particle injection flow rate, the measured particle count rates were normalized to the arbitrary selected count rate N1, which was measured for the suspension with a particle concentration (C1) and injected at the same flow rate. The count rates were found to vary linearly with the suspension particle concentration.

Hot Flow

This part of the study was undertaken to characterize the performance of the optical system in real combustion situations and to perform the necessary adjustments to the optical system for optimization of data acquisition. The adjustments to the receiving optics and to the power supplied to the photomultipliers were investigated and the reproducibility of the data was verified. Validation of and adjustments to the system are discussed below.

The combination of high intensity and number density of the signals obtained from sooting flames resulted in saturation of the signals sent to the ratio processor. This saturation may be interpreted as a result of the PMTs output consisting of current pulse values exceeding the input ratings of the dual-channel logarithmic amplifier. The latter has two ratings for pulse widths no less than 10 sec for current amplitudes as small as 1 nA, and pulse widths no less than 2 sec for amplitude as small as 1 A. The high output current was directly related to the high radiant flux of scattered light from the soot particles,

the radiant flux from the flame, and the power supplied to the PMTs. The dependence of the output current on the radiant flux and the PMT supply voltage can be expressed as

$$i=(F)(C)(10^{kE})$$

where E = supply voltage

F = radiant flux striking the cathode

and C and k are constants associated with a particular PMT.

Therefore, in order to reduce the high radiant flux striking the cathode of the photomultiplier tube, a mask having a 1-in diameter hole at the center was placed on each set of the receiving lenses. The amplitude and the frequency of the current pulse from the PMTs were thus diminished sufficiently to enable individual processing of the scattered signals from the soot particles.

Measurements of size and number density of soot particles were taken consecutively with and without the masks inside a propane flame. These results are presented in Figures 4-6 and 4-7 for size and number density measurements, respectively. The use of the masks on the receiving lenses had a dramatic effect on the soot particle number density but had only a slight effect on the size distribution.

The measured size distribution confirmed the computations conducted by Sterling (1986) on the independence of size measurement using the intensity ratioing technique upon collection solid angle. Sterling's results for scattering of light by soot particles are

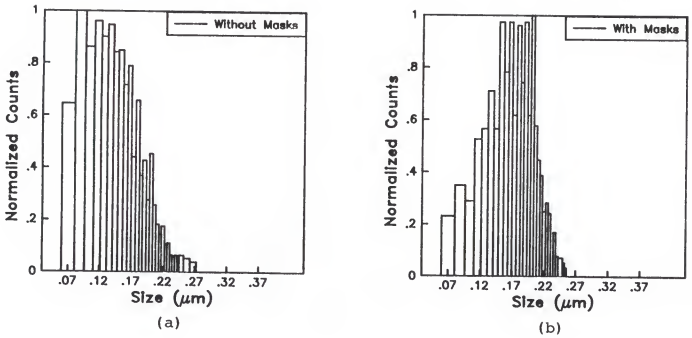

Figure 4-6a & b. Normalized Particle Count vs. Particle Site (a) without Masks, (b) with Masks on the Receiving Lenses.

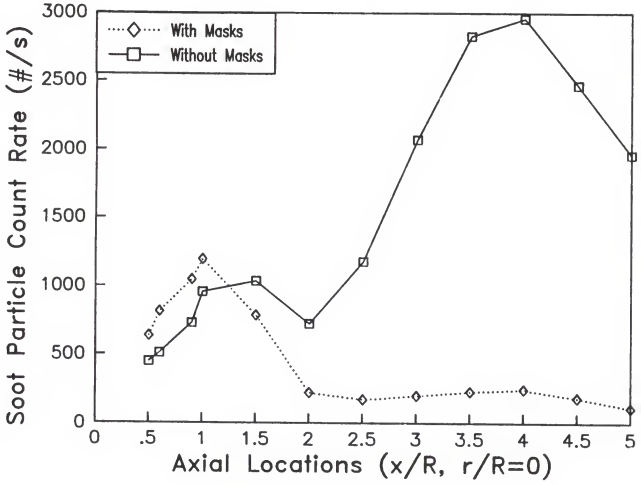

Figure 4-7. Soot Particle Count Rate at the Centerline With and Without Masks on the Receiving Lenses.

presented in Figure 4-8; they were obtained by direct calculations of the scattered intensities in the direction of the optical axis and by integrating the scattered intensities over the collecting lens aperture. The direct and integrated results were found to be nearly identical.

The soot particle number density was found to be higher inside the flame when the masks were used (Figure 4-7. The latter result was expected because of the attenuation of the radiant light striking the cathode. The soot number density outside the flame was found to be higher when the masks were not used. This result was also expected because the radiation flux from to the flame was almost absent, so only the laser scattered light from the soot particles struck the cathode of the PMTs.

Masking alone was not sufficient enough to reduce the amplitude and frequency of the signals from high sooting flames to an acceptable level for the ratio processor. Subsequently lowering of the voltages supplied to the PMTs afforded the necessary decrease in overall intensity and frequency of the current leaving the PMTs.

The voltages applied to the PMTs were decreased such that the size distribution at a point inside the flame stayed the same. Figure 4-9 presents the results of the voltages that had to be applied to the PMTs in order to obtain the same soot particle size distribution at a point far downstream of the flame, where the effect of the luminosity was negligible. The signal traces from the log-amplifier were monitored with a dual-trace oscilloscope.

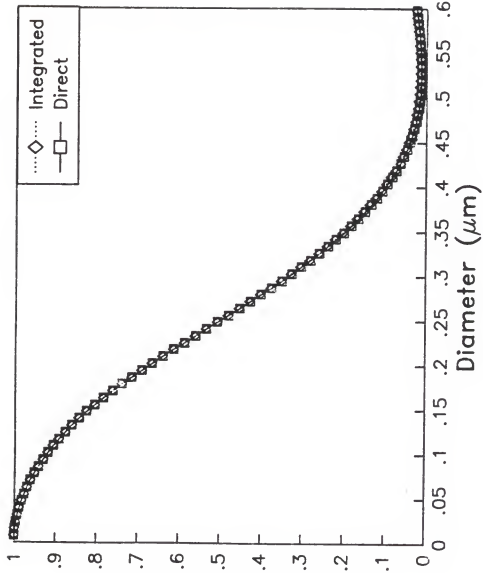

Figure 4-8. Calculated and Integrated Scattered Intensities vs. Particle Size.

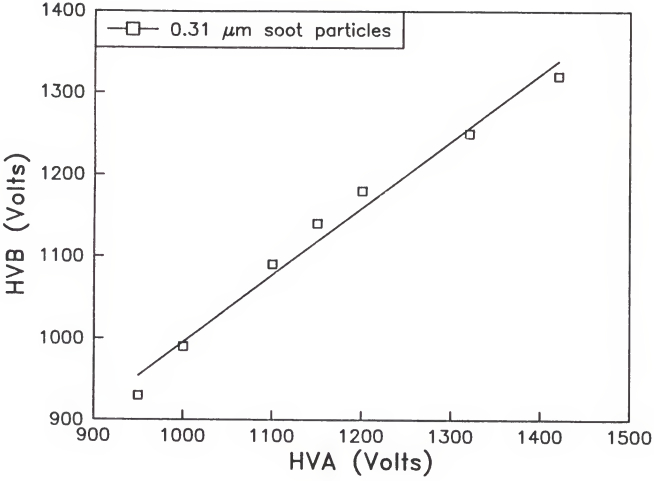

Figure 4-9. Applied Voltages on the Photomultiplier Tubes.

System Stability

The system stability was evaluated for a propene flame operating at an air/fuel mass ratio of 600 and an air velocity of 14 m/s. The data were taken at the same locations inside the flame on two different days. The results, presented in Figure 4-10, show an adequate reproducibility of the data with a maximum error of about 10%.

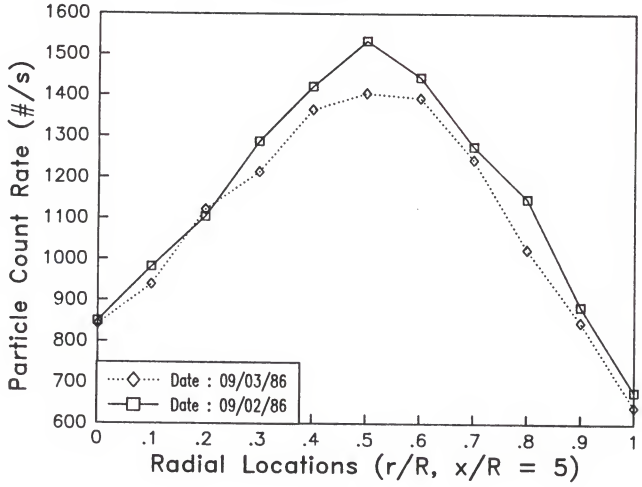

Figure 4-10. Reproducibility of Data for a Propene Flame.

CHAPTER V
SOOT MORPHOLOGY AND CHEMICAL ANALYSIS OF PAHs ADSORBED ON THE SOOT PARTICLE SURFACE

Soot Morphology

A morphological analysis of different soot samples collected from different fuels was attempted using a Scanning Electron Microscope (SEM). The soot samples were collected on 47-μm Nuclepore membrane filters with 0.2-μm pore size. The soot particles collected consisted of agglomerate whith chain-like structure with diameters up to 1 μm and small individual spherules with diameters less than 0.1 μm (Figure 5-1). The size and the shape of the soot aggregates collected on the filters are consistent with what it is reported in the litterature; however, the collection time t_c on the filter was found to affect the shape of the soot particles collected. A long collection time led to a greater extent of aggregation of the soot particles on the Nuclepore filters, distorting the information concerning the real size and shape of the soot particle aggregate inside the flame.

Figure 5-1 shows photographs of two soot samples collected from the same acetylene flame but at two different sampling times. The degree of soot aggregation was found much greater in the sample which gathered during the longer collection time. Therefore, smaller collection

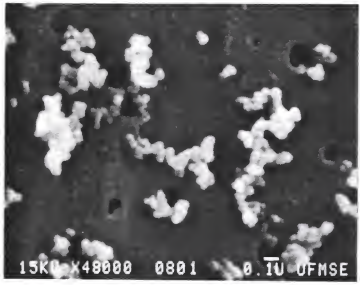

(a) t = 3s

(b) t = 5s

Figure 5-1. S.E.M. Photographs of Two Soot Samples Obtained from the Same Acetylene Flame but at Two Different Collection Times.

collection times (approximatively 3 seconds) were used for soot morphology analysis.

Soot samples from four flames operating with four different fuels (propane, 1-butene, isobutylene, and acetylene) were characterized by electron microscopy with a total magnification of 40,000 and 48,000. Photographs from each sample are presented in Figure 5-2. As expected, the soot aggregate size and number density for the propane flame were observed to be much smaller than those found in other flames. At equivalent collection times, the soot aggregates from the acetylene flame exhibit a more elongated chain-like structure than the others. Morphology of the soot collected from the different flames suggests that the aggregates were formed from a multitude of spherules.

Chemical Analysis of PAHs Collected on the Soot Surface

Polycyclic aromatic hydrocarbons (PAHs) formed as products of incomplete combustion of organic fuels are a potential health hazard because of their toxicity. An understanding of the chemical pathways leading to formation of soot, which is composed of these combustion products, would be of considerable value in understanding the phenomena leading to soot formation. Characterizing the chemical mechanism of soot formation is an active subject of research in its own right (chapter 2), and this report will present some observations on the chemical composition

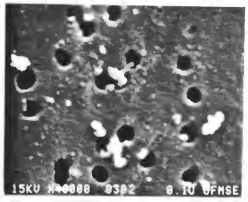

(a)

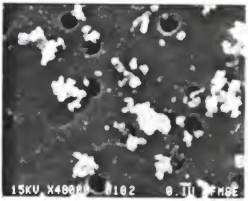

(b)

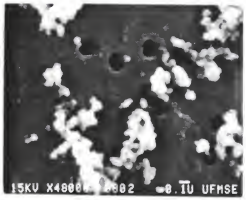

(c)

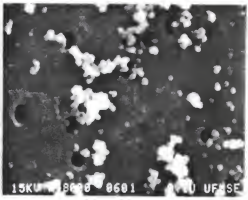

(d)

Figure 5-2. S.E.M. Photographs of Soot Samples Obtained from (a) Propane; (b) 1-Butene; (c) Isobutylene; (d) Acetylene.

of PAHs extracted from soot samples, without speculations about the mechanistic processes involved in their formation.

Samples of soot were obtained from two locations: on the face of the burner, and on a filter (Figure 3-4) located in the exhaust system, about six feet downstream of the burner. The filter used is one half of a Schleicher and Schull binder-free quartz micro-fiber 8x10 inch filter. The filters were conditioned in an oven at 400°C for 4 hours, cooled, weighed and stored in a dessicator prior to use. Three runs were conducted at air/fuel ratio of 800, in which pure fuels (Propane, propene, and 1-butene, respectively) were burned. At the end of each run, soot samples were collected from the burner face and the filter.

The samples were stored at 0°C until they were extracted for 24 hours with methylene chloride in a Soxhlet apparatus (Whatman 33 x 80 mm single thickness cellulose thimbles with a light glass wool plug at the top). The glass wool and thimbles were periodically pre-extracted whith the methylene chloride, dried at 50°C and 3 torr, and tared. The solvant volume for extraction was approximatively 250 ml with a cycle time for extraction of about 6 minutes. After extraction, the soluble materials were concentrated to 5.0 ml in a Kuderna--Danish apparatus, at 98°C in a water bath. Gas chromatographic analyses were carried out using a Perkin--Elmer Sigma 2000 instrument fitted with a J and W Scientific 30 m, 250 m open tubular column with walls of which was bounded a 0.1- m film of

DB-5. Eluting components were "visualized" using a flame ionization detector (FID). The injection mode was 30:1 split ratio and the linear velocity of helium through the column was 35 cm/sec at 100°C. The injection port and the detector were maintained at 300°C. The oven temperature was initially set at 50°C and was gradually increased to 125°C at a rate of 5°C/min and then increased to 300°C at 8°C/min, with a 10 minutes final temperature hold. The sample volumes injected were 1 or 2 l.

The analyses of the extracts from soot particles amounts to a study of complex mixtures. Identification of some of the components of the mixture were made on the basis of retention time. The retention times were obtained for standards (pure compounds) which were analyzed using the same capillary column and operating conditions used for exhaust emission analyses.

Some of the PAHs identified by retention times in this experiment are presented in table 5-1 for all the soot samples collected .

Chromatograms of the products extracted from different soot samples collected on the filter are presented in Figure 5-3. The chromatograms for the extractable products were qualitatively identical for all three flames studied, suggesting that, under the conditions of this study, the PAHs collected on the filter reached their final state which is independent of the parent fuel burned.

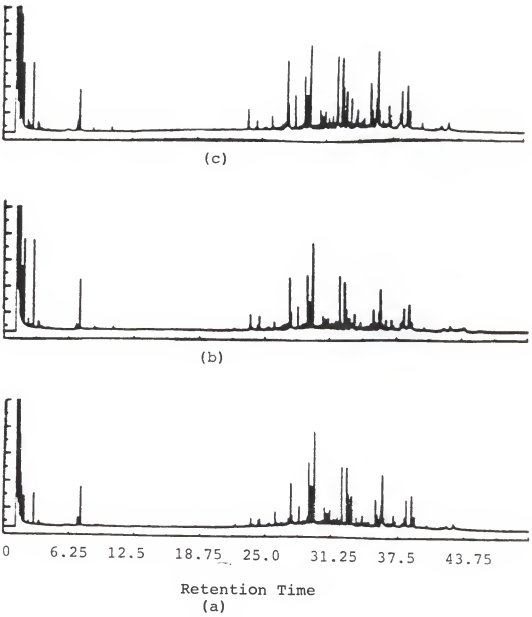

Figure 5-3. Chromatograms of Chemical Products Extracted from Soot Sample Collected on a Filter: (a) Propane Flame; (b) Propene Flame; (c) Isobutene Flame.

Representative chromatograms of the extractable volatiles present in soot collected at the face of the burner (Figure 5-4) show significant qualitative differences in composition. These products were trapped before reaching chemical equilibrium, because the face of the burner provides a mechanism for premature termination of the polymerization reactions of intermediates present during the various steps of the combustion process. The differences in the distribution of intermediate products suggests that the polymerization process shows some specifity to the parent fuel during the early stages; however, the similarity in the compositions of products isolated from the exhaust stream suggests that these different chemical pathways ultimately converge to a common distribution of equilibrium products that is independent of the fuel structure.

The above are consistent with the operation of multiple, convergent pathways rather than one chemical mechanism leading to the formation of high molecular weight PAHs and soot and asserts the complexity involved in exact modeling of soot formation processes.

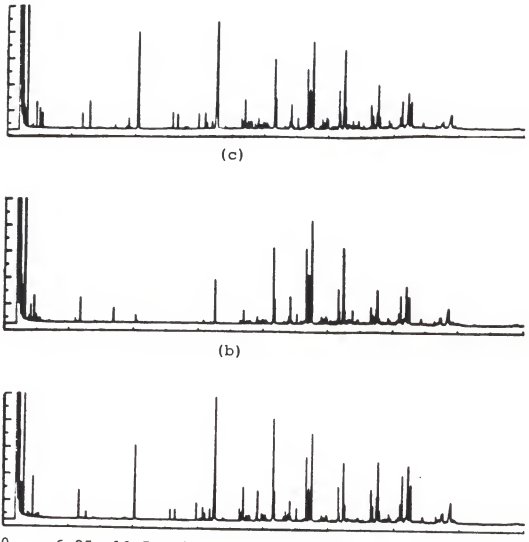

Figure 5-4. Chromatograms of Chemical Products Extruded from Soot Samples Collected on the Face of the Burner: (a) Propane Flame; (b) Propene Flame; (c) Isobutene Flame.

TABLE 5

Identification by retention times of some polycyclic aromatic hydrocarbons in combustor soot samples

Sample	Retention Time	Area	Identification
(Propene) Filter	30.87	1532	Benzo(b)fluorene
	32.87	7504	Triphenylene
	34.03	1113	Benzo(a)anthracene
	35.98	21414	Benzo(e)pyrene
	36.15	3372	Benzo(a)pyrene
	38.73	17738	Benzo(ghi)pyrene
	42.66	4521	Coronene
(Peaks present: 31; Peaks identified: 7)			
(Propene) Scraping	12.73	6148	Napthalene
	20.39	39104	1-5 Dimethylnapthalene
	30.87	3696	Benzo(b)fluorene
	32.81	82636	Triphenylene
	34.07	2319	Benzo(a)anthracene
	35.41	15870	Benzo(k)fluoranthene
	35.92	15742	Benzo(e)pyrene
	36.10	2047	Benzo(a)pyrene
	42.89	35700	Coronene
(Peaks present: 33; Peaks identified:9)			
(Propane) scraping	12.82	393314	Naphtalene
	16.60	27449	Azulene
	30.89	5756	Benzo(b)fluorene
	32.86	301390	Triphenylene
	34.05	9155	Benzo(a)anthracene
	35.37	52578	Benzo(b)fluoranthene
	36.07	108229	Benzo(a)pyrene
	38.34	85756	Indeno(1,2,3,cd)pyrene
(Peaks present: 58; Peaks identified: 8)			

TABLE 5 (Continued)

Sample	Retention Time	Area	Identification
(Propane)	20.33	1337	1,5 Dimethylnapthalene
Filter	29.92	1079	Pyrene
	30.89	15140	Benzo (b) fluorene
	32.84	18989	Triphenylene
	33.09	3473	Chrysene
	34.01	4269	Benzo(a)anthracene
	35.94	37799	Benzo(k)fluoranthene
	36.08	92952	Benzo(a)pyrene
	38.32	45467	Indeno(1,2,3,cd)pyrene
	42.78	23262	Coronene
(Peaks present: 40; Peaks identified: 10)			
(1-Butene)	12.67	78230	Napthalene
scraping	16.07	10661	Azulene
	20.36	194765	1,5 Dimethylnapthalene
	29.38	30394	Fluoranthene
	30.84	2852	Benzo(b)fluorene
	32.84	14168	Triphenylene
	34.06	3178	Benzo(a)anthracene
	35.92	12416	Benzo(e)pyrene
	36.10	3476	Benzo(a)pyrene
	38.80	25319	Indeno(1,2,3,cd)pyrene
(Peaks present: 28; peaks identified: 10)			
(Butene)	26.30	1730	Anthracene
Filter	29.92	1213	Pyrene
	30.86	7616	Benzo(b)fluorene
	32.82	13651	Triphenylene
	35.34	22683	Benzo(b)fluoranthene
	35.99	616516	Benzo(e)pyrene
	36.13	10107	Benzo(a)pyrene
	38.33	1359	Indeno(1,2,3,cd)pyrene
	42.90	59110	Coronene
(Peaks present: 37; Peaks identified: 9)			

CHAPTER VI
EXPERIMENTAL RESULTS AND DISCUSSION

Introduction

A series of experiments were implemented to study the key physico-chemical parameters that control the formation, growth, and oxidation processes of soot particles in a well-defined combustor configuration. It has been argued that formation and evolution of soot particles in flames is controlled by competition between the rate of pyrolysis of the parent fuel and the rate of oxidation of the soot precursors and the formed soot particles (Milliken, 1962). The rates of pyrolysis of fuel and the oxidation of the soot precursors and soot particles are temperature-dependent. This requires that they be considered functions of interrelated parameters such as fuel structure, residence time, rate of mixing of the fuel with the potential oxidants, and fuel heat content, which, in turn are determined by the operating conditions. The separate effects of these parameters on the fate of a soot particle was examined using a selective set of independent parameters. The controlling parameters that were investigated in this study are: fuel type, fuel flow rate, fuel heat content, air/fuel ratio, and air and fuel jet velocities.

This chapter is divided into four parts. The first part deals with the operating conditions and the reasoning behind their selection. The second part is a succinct summary of a companion project performed by Roe (1987) on flow field mapping of a similar combustor. In the third part, the experimental results for temperature distributions are presented. The final part contains the experimental results and a discussion of soot formation and oxidation processes in the present study.

Experimental Conditions

Soot emissions are intimately related to the heat transfer, aerodynamics, and chemical processes that occur in flames. Although these processes are interrelated, they were investigated separately because simultaneous measurements in flames are very difficult to achieve. Different operating conditions were implemented to investigate the main parameters that affect the temperature distribution, the particle velocity distribution, and the chemical mechanisms that affect soot production in flames.

The Integrated Particle Sizing System (IPSS) and the Laser Doppler Velocimeter (LDV) (Roe, 1987) were used to characterize the soot particle and velocity fields, respectively. Fine wire thermocouples were used to measure the temperature distribution in flames. The data inside the flames were taken at different locations; locations are expressed as the dimensionless ratio of displacement from

centerline to the radius R of the bluff body of the burner. The radial profiles of soot yield were taken for one axial location (x/R = 3) outside the flames.

The experimental work involving measurement of soot particle size and flux rates, temperature, and velocity distributions was divided into four sets of experiments. First, measurements were performed for a number of flames in which the fuel flow rate and fuel species were varied (Table 6-1). Second, a set of measurements was obtained for flames in which nitrogen was added to the fuel to maintain a constant fuel jet velocity (Table 6-2). The latter was designed to show the effect of the fuel flow rate on soot formation in flames operating with similar flow conditions. Third, a set of experiments (Table 6-3) was designed to demonstrate the temperature effect on soot formation. Nitrogen was added in graduated proportions to different fuel species to maintain a constant total heat content of the fuel stream while varying the fuel jet velocity. The final set of experiments was designed to investigate the effect of nitrogen dilution on soot field (Table 6-4). Each set of experiments was investigated for three fuels (propene, 1-butene, and isobutylene).

Velocity Measurements

Flowfield mapping of different flames was undertaken by Roe (1987) using a combustor similar to the one used in this investigation. Velocity mapping was used to characterize flow fields behind a bluff-body burner for

TABLE 6-1

Flow Conditions for Experiment No. I (Effect of Fuel Flow Rate)

Experiment[1] No.	Fuel	Flow rate (cm^3/s)	Velocity (m/s)	Air/Fuel Ratio
I1	Propene	20.42	13.9	1200
I2	Propene	24.51	16.6	1000
I3	Propene	30.63	20.8	800
I4	Propene	40.85	27.7	600
I5	Propene	61.27	41.6	400
I6	1-Butene	15.28	10.4	1200
I7	1-Butene	18.34	12.4	1000
I8	1-Butene	22.92	15.6	800
I9	1-Butene	30.66	20.8	600
I10	1-Butene	45.84	31.1	400
I11	Isobutylene	15.85	10.8	1200
I12	Isobutylene	19.02	12.9	1000
I13	Isobutylene	23.77	16.1	800
I14	Isobutylene	31.70	21.5	600
I15	Isobutylene	47.54	32.3	400

[1]The air reference velocity for this set of experiments is maintained constant at a value of 14 m/s.

TABLE 6-2

Flow conditions for Experiment No. II (Constant Fuel Jet Velocity)

Experiment No.	Fuel	Fuel Flow Rate (cm^3/min)	Nitrogen Flow Rate (cm^3/min)	Nitrogen/Fuel Velocity (m/s)	Nitrogen/Fuel Ratio %
II1	Propene	55.19	9.20	49.9	10
II2	Propene	49.05	18.40	49.9	20
II3	Propene	42.92	27.59	49.9	30
II4	Propene	36.79	36.79	49.9	40
II5	Propene	30.65	46.01	49.9	50
II6	1-Butene	41.89	9.28	42.1	10
II7	1-Butene	37.23	18.67	42.1	20
II8	1-Butene	32.58	28.01	42.1	30
II9	1-Butene	27.92	37.28	42.1	40
II10	1-Butene	23.27	46.62	42.1	50
II14	Isobutylene	43.47	9.28	43.2	10
II15	Isobutylene	38.64	18.64	43.2	20
II16	Isobutylene	33.81	27.97	43.2	30
II17	Isobutylene	28.98	37.26	43.2	40
II18	Isobutylene	24.15	46.60	43.2	50

TABLE 6-3

Flow Conditions for Experiment No. III (Constant Heat Release)

Experiment[1] No.	Fuel	Fuel Flow Rate (cm^3/s)	Nitrogen Flow Rate (cm^3/s)	Nitrogen/Fuel Velocity (m/s)
III1	Propene	42.30	0.00	28.7
III2	Propene	42.30	18.40	44.4
III3	Propene	42.30	23.58	47.2
III4	Propene	42.30	28.77	50.0
III5	Propene	42.30	37.73	54.9
III6	Propene	42.30	45.28	59.0
III7	1-Butene	30.66	0.00	20.8
III8	1-Butene	30.66	17.92	35.8
III9	1-Butene	30.66	23.11	38.2
III10	1-Butene	30.66	28.30	40.5
III11	1-Butene	30.66	39.15	45.4
III12	1-Butene	30.66	46.70	48.8
III13	Isobutylene	32.21	0.00	21.9
III14	Isobutylene	32.21	19.81	38.0
III15	Isobutylene	32.21	25.00	40.4
III16	Isobutylene	32.21	30.19	42.8
III17	Isobutylene	32.21	39.15	46.9
III18	Isobutylene	32.21	46.70	50.4

[1] The air velocity and the the heat release rate were maintained equal to 14 m/s and 196 Btu/min, respectively.

TABLE 6-4

Flow Conditions for Experiment No. IV (Air Reference Velocity Effects)

Experiment No.	Fuel	Fuel Flow Rate (cm^3/s)	Fuel Velocity (m/s)	Air Flow Rate (dm^3/s)	Air Velocity (m/s)
IV1	Propene	40.85	27.7	26	10
IV2	Propene	40.85	27.7	31	12
IV3	Propene	40.85	27.7	36	14
IV4	Propene	40.85	27.7	41	16
IV5	1-Butene	30.56	20.7	26	10
IV6	1-Butene	30.56	20.7	31	12
IV7	1-Butene	30.56	20.7	36	14
IV8	1-Butene	30.56	20.7	41	16
IV9	Isobutylene	31.7	21.5	26	10
IV10	Isobutylene	31.7	21.5	31	12
IV11	Isobutylene	31.7	21.5	36	14
IV12	Isobutylene	31.7	21.5	41	16

both reacting and non-reacting flows. The operating conditions were set in an overall program at the university of Florida Combustion Laboratory (UFCL) to investigate the relationship between flow field and soot formation. A summary of Roe´s work to characterize flowfields behind a bluff-body burner is given next.

Flame velocities were determined using a Laser Doppler Velocimeter (LDV) operating in backscatter mode. The system consists of a 4-W argon-ion laser and a TSI Inc. modified back scattered 9100-6 modular optical assembly. The system is described in detail by Roe (1987).

Roe conducted pure fuel tests at air/fuel mass ratios of 800 and 400 as well as at very rich (A/F = 175) and lean condition (A/F = 6000) for propene flames. A non-reacting nitrogen jet at a mass ratio air/nitrogen of 400, a nitrogen-diluted propene flame and a butene flames were investigated. A typical flowfield plot for a 1-butene flame operating at an air/fuel mass ratio of 800 is shown in Figure 6-1. The flowfield pattern consists of a single recirculation vortex between the fuel nozzle and the centerbody outer diameter; there is no significant crossflow along the centerline.

According to Roe, the fuel jet flow rate does not dominate the flowfield pattern within the range tested. It was observed that a 10-fold increase in the heat content of the fuel stream caused no significant change in flow pattern or recirculation zone; however, a significant

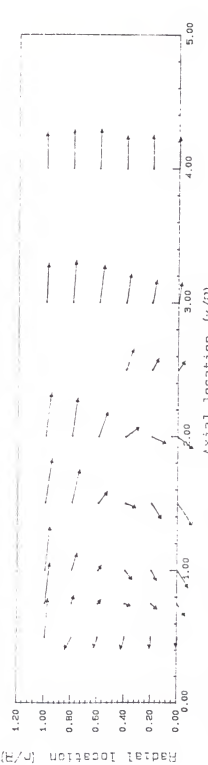

Figure 6-1. Flowfield for 1-Butene Flame Operating at A/F = 800.

change in the flow patterns was observed between reacting and non-reacting flows. A relatively small increase in the heat content of the fuel stream was seen to increase radial outflow near the face of the burner, increase axial inflow throughout the recirculation zone, expand the recirculation region radially, and lengthen the recirculation zone axially from 1.8 radii for a non-reacting flow to 2.2 radii for a reacting flow. Roe concluded that the effect of a small amount of energy release is more significant than the fluid mechanics of a non-reacting fuel jet to the experiments conducted.

The conclusions that can be drawn from Roe's work on velocity measurements behind a bluff body burner can be summarized as

- The flowfield pattern was found to be a characteristic of the burner configuration.
- A significant change in the flow pattern between reacting and non-reacting flows was observed.
- The fluid mechanical and the heat content of the fuel stream (for reacting flows) exert only a marginal effect on the flowfields.

Temperature Measurements

Flame temperature was recognized by several workers (Glassman and Yaccarino, 1981; Gomez et al., 1984) as an important parameter in determining the sooting tendency of different fuel species. The sooting process as postulated by Milliken (1962) is a competitive process between the rates of pyrolysis-forming and oxidation-consuming of the soot precursors. The relative importance of these

processes is temperature dependent. This coupling between the sooting process and temperature in flames forms the basis of the present study which examines different parameters that affect the temperature field.

Fuel Flow Rate

The effects of fuel flow rate and fuel species on flame temperature fields were investigated for a series of flames in which the fuel flow rate and fuel species were varied (Table 6-1) for the flow conditions for the flames studied). Temperature measurements for these flames are presented in Figures 6-2, 6-3, and 6-4. The maximum measured temperatures for each flame were observed to increase with the fuel flow rate. At all axial locations the maximum measured temperatures were found to be located in the vicinity of the centerline. Further, the peak temperatures occur at an axial location about 1.6 bluff-body radii downstream. This location corresponds approximatively to the region where the flow changes direction (Figure 6-1). This region separates the hot products and cool air moving downstream from the recirculated hot products and reactants moving upstream. The hot products moving upstream entrain and heat up the fuel as it is injected in the combustion zone.

The high temperatures observed in the vicinity of the centerline are due to the relatively long mixing time of the fuel with the recirculating hot products because of the low velocities existing in this region. Another high

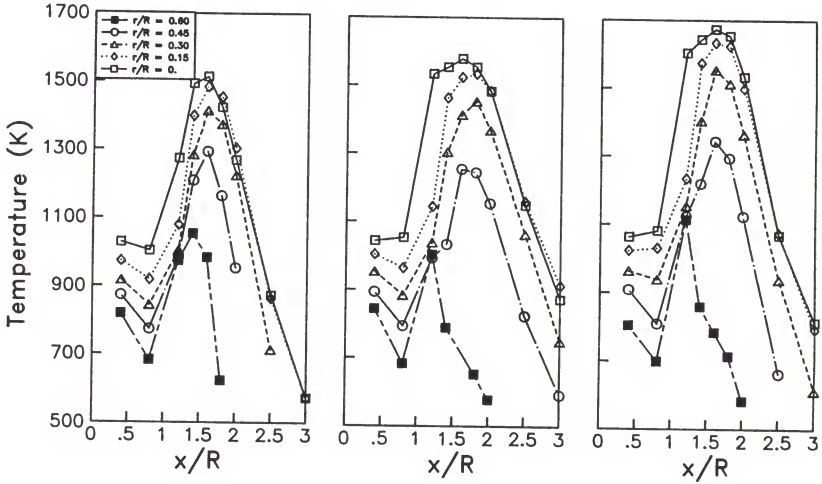

Figure 6-2. Temperature Distributions for Propene Flames Operating at Different Air/Fuel Mass Ratios: (a) A/F = 800; (b) A/F = 600; (c) A/F = 400.

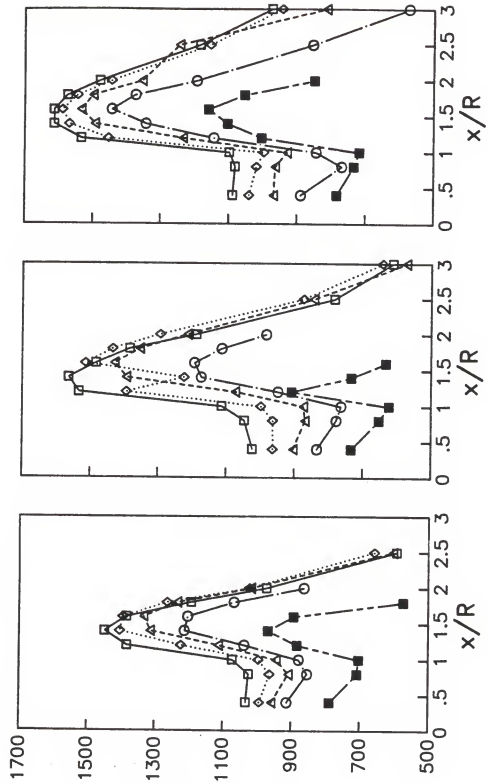

Figure 6-3. Temperature Distributions for 1-Butene Flames Operating at Different Air/Fuel Mass Ratios: (a) A/F = 800; (b) A/F = 600; (c) A/F = 400.

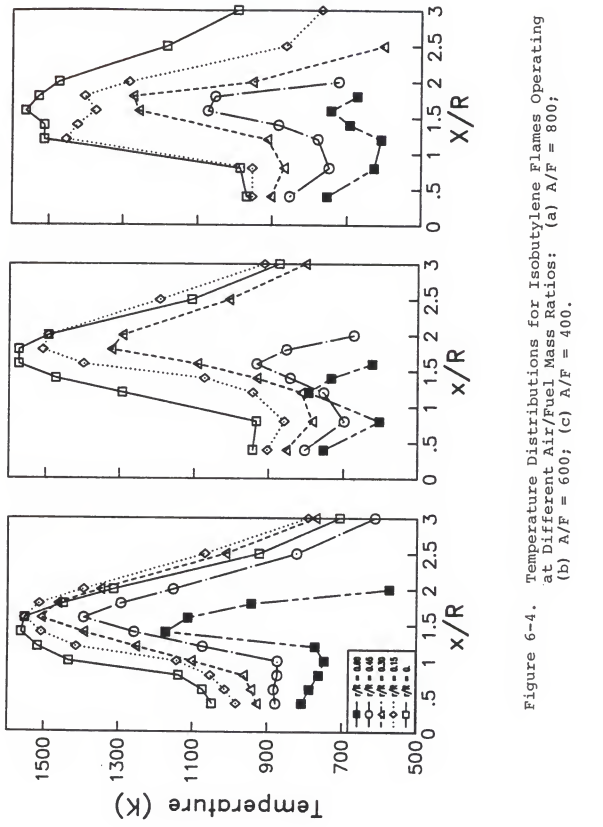

Figure 6-4. Temperature Distributions for Isobutylene Flames Operating at Different Air/Fuel Mass Ratios: (a) A/F = 800; (b) A/F = 600; (c) A/F = 400.

temperature region should be expected near the vortex center established by the annular air jet; however, the measured temperatures in this region were observed to be much lower than the temperatures at the centerline. This can be attributed to different factors: a) the high soot loading in this region might have distorted the thermocouple measurements; b) the measured temperatures are an average that includes the cool annular air flow; c) the chemical reactions take place in small structures or vortices shed by the fuel jet (next); because of the large air/fuel ratios of the type of flames under investigation in this work, one can speculate that most of these vortices are located in the outer shear layer of the fuel jet and that most of the reactions take place before the fuel reaches the annular air jet vortex. This last explanation seem to be accurate because numerous attempts to locate high temperatures in the annular vortex were unsuccessful.

To explain why an increase in the fuel flow rate results in higher flame temperatures and to interpret some other phenomenom observed throughout this study, one needs to "visualize" the mixing process occurring in turbulent reacting flows. According to Magnussen (1981), the rate-controlling phenomenon for reactant consumption in turbulent reacting flames is the molecular mixing that occurs within some fine structures believed to be vortex tubes, sheets, or slabs. These fine structures are localized at the interface of larger structures (eddies)

produced by the interaction of the recirculating flow and the fuel jet streams. The kinetic energy lost from the larger eddies is transferred to the smaller eddies which dissipate that energy as heat.

In the case under study, velocity measurements have shown that the fluid mechanics and the heat content of the fuel stream exert only a marginal effect on the flowfield. Therefore, an increase in the fuel flow rate mainly increases the fuel/air ratio of the big eddies and subsequently increases the diffusion of fuel from the fuel-rich eddies into the fine structures where chemical reactions take place. Indeed, an increase in the fuel flow rate would increase the local fuel ratios inside the fine structures resulting in higher flame temperatures. The fine structures provide a medium characteristic to premixed gases where both fuel and oxygen are present.

Furthermore, at equivalent global air/fuel mass ratios, the fuel having higher heat content produced higher flame temperatures. This was expected since the heat release rate from the combustion of fuel is linearly dependent on the fuel stream heat content which includes both the effect of fuel flow rate and fuel heat content. The heat content of the fuel stream can be considered as a potential parameter in correlating the sooting tendencies of fuels.

Fuel Stream Heat Content

As stated previously the flame temperature was directly related to the local air/fuel ratios inside the fine structures surrounding the big eddies. Therefore, the flame temperature is also dependent on the oxygen concentration in these fine structures. Glassman and Yaccarino (1981) concluded from their work with a diffusion flame that an increase in the fuel jet velocity would induce more air on the fuel side as the flame is lifted further off the burner. Therefore, the fuel jet velocity is a parameter to be considered in the temperature field study. The latter observation prompted a second set of experiments (Table 6-2), in which nitrogen dilution of the fuel flow was done to achieve a constant fuel jet velocity while varying the fuel flow rate. This set of experiments was designed to separate the effect of fuel stream heat content (defined as the product of the fuel flow rate and the fuel heat content) from fuel jet velocity.

The results of these experiments are shown in Figures 6-5, 6-6, and 6-7 for flames fueled by propene, 1-butene, and isobutylene, respectively. The results were found to follow the same trend as the ones obtained in the first set of experiments; higher fuel flow rates and fuel stream with higher heat content resulted in higher flame temperatures. Given that the aerodynamics of the flame for this specific burner is essentially controlled by the air jet velocity (above), the effect of the fuel jet velocity

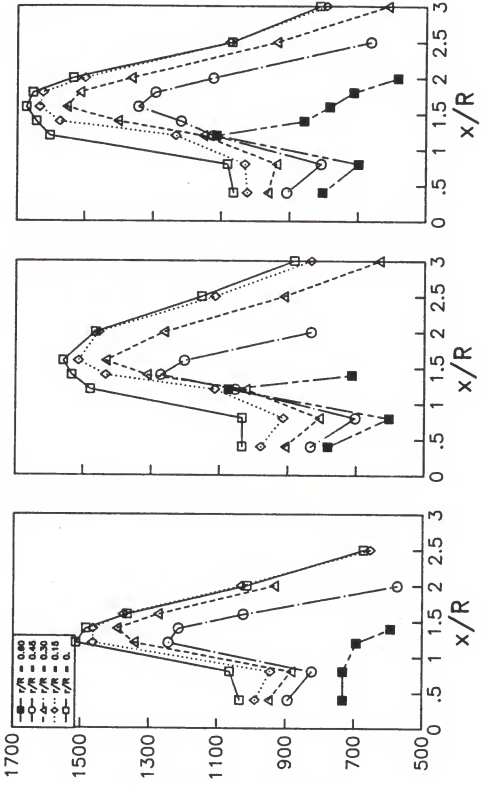

Figure 6-5. Temperature Distributions for Propene Flames Operating at Different Air/Fuel Mass Ratios: Fuel/Nitrogen Mass Flow Rate Constant: (a) A/F = 800; (b) A/F = 600; (c) A/F = 400.

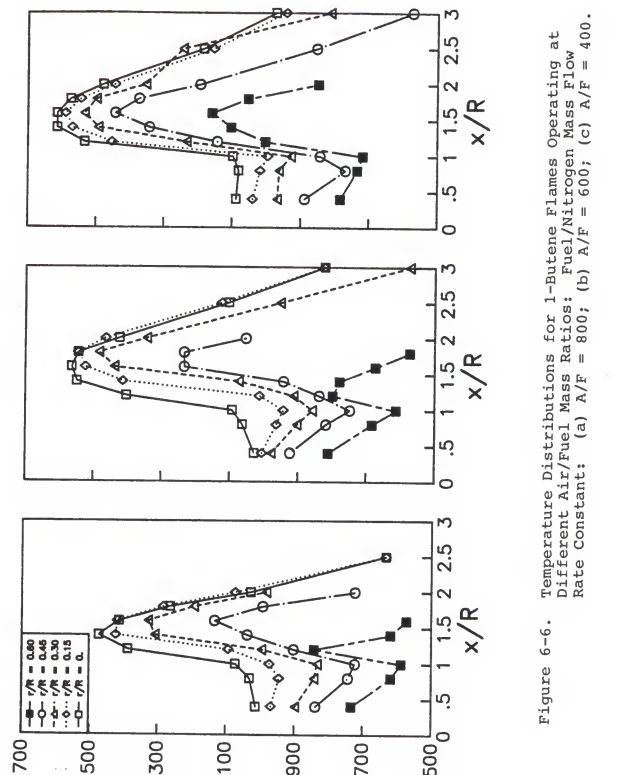

Figure 6-6. Temperature Distributions for 1-Butene Flames Operating at Different Air/Fuel Mass Ratios: Fuel/Nitrogen Mass Flow Rate Constant: (a) A/F = 800; (b) A/F = 600; (c) A/F = 400.

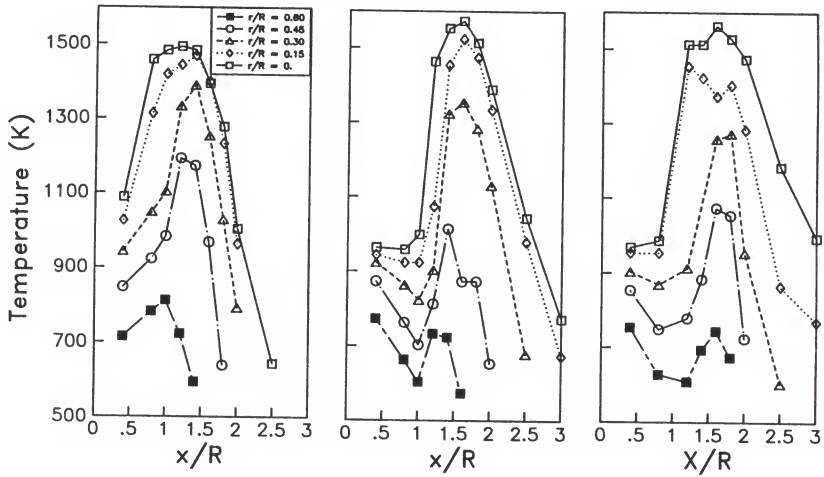

Figure 6-7. Temperature Distribution for IsoButylene Flames Operating at Different Air/Fuel Ratios: Fuel/Nitrogen Mass Flow Rate Constant: (a) A/F = 800; (b) A/F = 600; (c) A/F = 400.

could be thought to be only a marginal determinant of the temperature field under the conditions set for these experiments; however, this effect could not be clearly determined because the fuel stream heat content in experiments I and II, and nitrogen dilution in experiment II have a direct effect on the flame temperatures. Indeed, both sets of experiments discussed above show that an increase in the fuel flow rate or in the fuel heat content contibute directly to an increase in the flame temperatures.

Nitrogen Dilution

An alternative approach to varying the temperature field of the flames is maintaining the total fuel stream heat content constant while varying the fuel jet velocity . This set of experiments was developed to examine the nitrogen dilution effect on the flame temperature. The operating conditions for this set of experiments are presented in Table 6-3. The fuel flow rates were kept constant while nitrogen was added progressively to the fuel stream. The temperatures measured in these experiments are presented in Figures 6-8, 6-9, and 6-10 for propene, 1-butene, and isobutylene flames, respectively. The results show that nitrogen dilution resulted in a relatively small increase in the flame temperatures downstream of the flame. Decreased soot production was observed in the formation region as the nitrogen flow rate was increased,

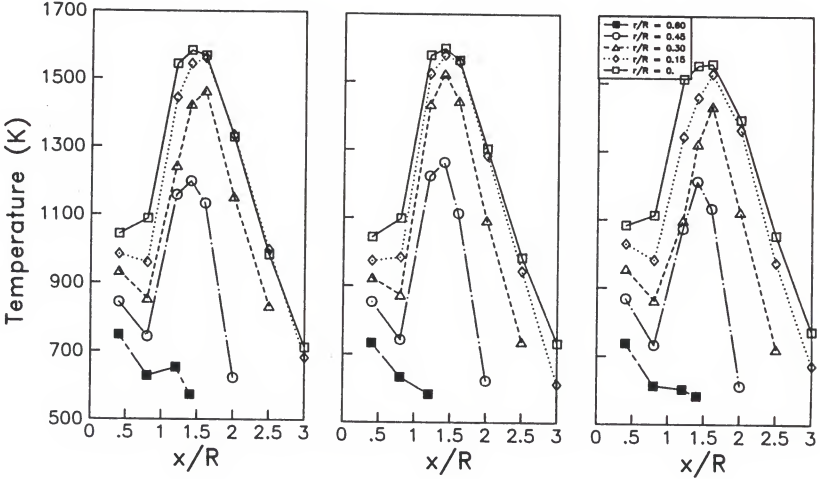

Figure 6-8. Temperature Distributions for Nitrogen Diluted Propene Flames (Nitrogen added: (a) 18.4 cm^3/s; (b) 23.6 cm^3/s; (c) 28.8 cm^3/s).

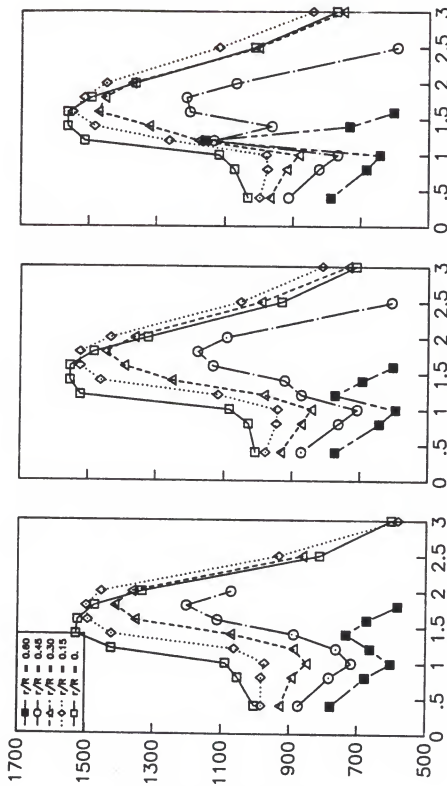

Figure 6-9. Temperature Distributions for Nitrogen Diluted 1-Butene Flames (Nitrogen added: (a) 18.4 cm^3/s; (b) 23.6 cm^3/s; (c) 28.8 cm^3/s).

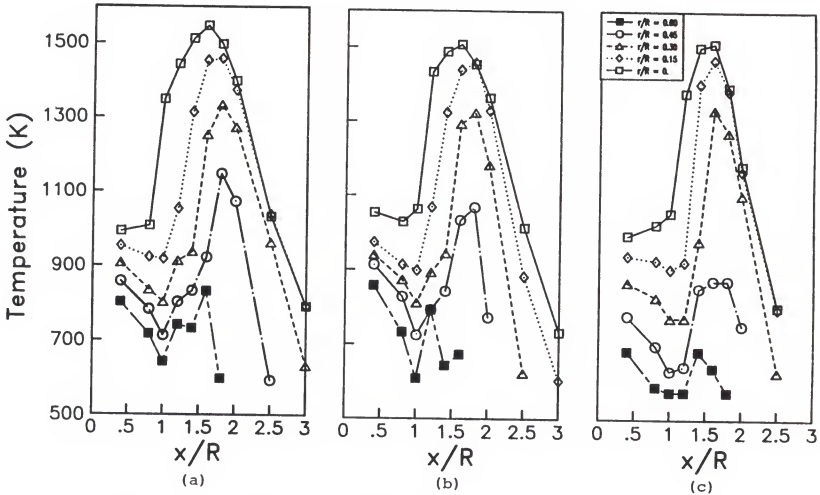

Figure 6-10. Temperature Distribution for Nitrogen Diluted IsoButylene Flames (Nitrogen added: (a) 18.4 cm^3/s; (b) 23.6 cm^3/s; (c) 28.8 cm^3/s)

and diminished radiative losses may have contributed to the high temperatures observed downstream the flame.

Air Reference Velocity

The last set of experiments (Table 6-4) related to temperature examined the influence of the air reference velocity. The results are presented in Figures 6-11, 6-12, and 6-13 for propene, 1-butene, and isobutylene flames, respectively; however, the data in these figures do not reveal a characteristic effect of the air velocity on the temperature field. An increase in the air velocity could decrease or lean out the rich fuel eddies; however, the air jet momentum is much larger than the fuel jet momentum, and an increase in the air velocity probably would not affect the characteristics of the big eddies. An increase in the air velocity resulted in cooler flames, most likely owing to higher convective losses from the flame to the air jet.

The experimental results obtained from investigation of the flame temperature studies behind a bluff body burner can be summarized as follows:

- The flame temperature is a strong function of the heat release rate.
- The fuel and air jet velocities exert only a marginal effect on the temperature field.
- The soot loading affects the temperature field.

Soot Measurements

The soot particle size and population density measurements were made using the Integrated Particle Sizing

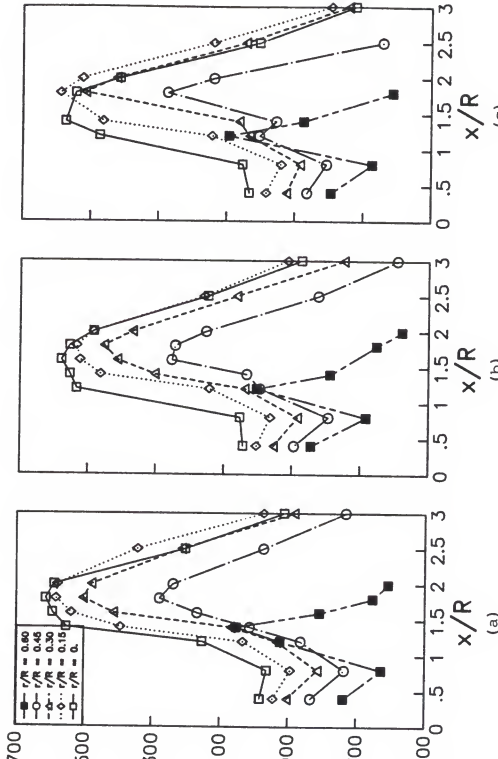

Figure 6-11. Temperature Distributions for Propene Flames Operating at Different Air Reference Velocities: (a) v = 12 m/s; (b) v = 14 m/s (c) v = 16 m/s.

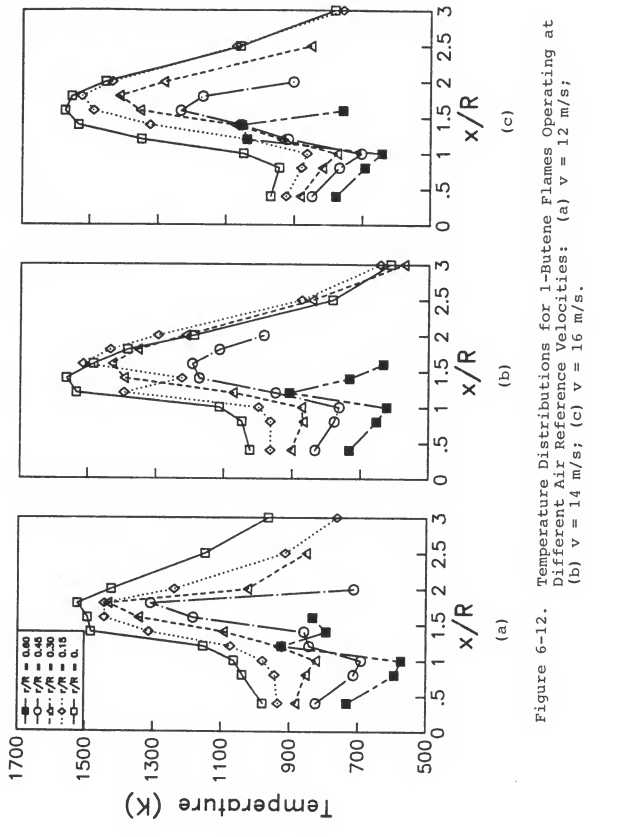

Figure 6-12. Temperature Distributions for 1-Butene Flames Operating at Different Air Reference Velocities: (a) v = 12 m/s; (b) v = 14 m/s; (c) v = 16 m/s.

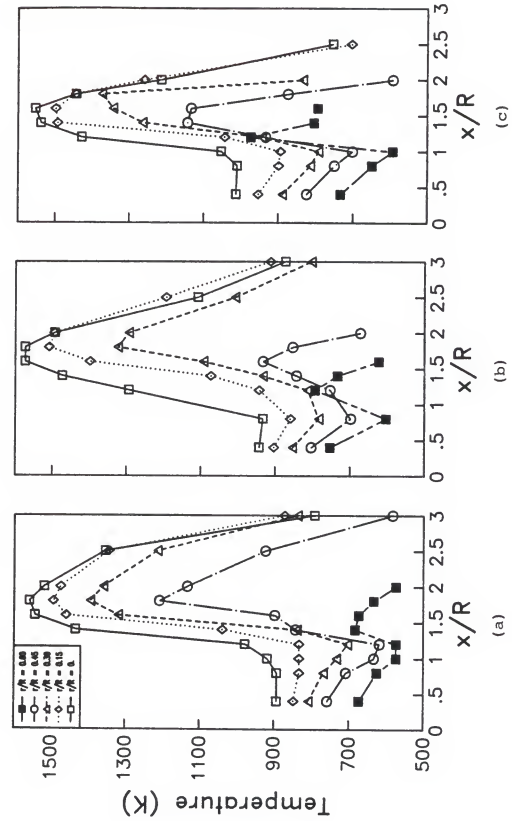

Figure 6-13. Temperature Distributions for IsoButylene Flames Operating at Different Air Reference Velocities: (a) v = 12 m/s; (b) v = 14 m/s; (c) v = 16 m/s.

System (IPSS). As said earlier, The sooting process is the results of interrelated processes that involves chemistry, heat transfer, and fluid mechanics inside a flame. This section is divided in three parts: In the first part, the relationship between soot and velcity fields will be presented. In the second part, the sooting field will be investigated with respect to the effect of fuel flow rate, heat release rate, fuel jet velocity, and air reference velocity. Further, the relationship between the soot, velocity, and temperature fields will be assessed. In the last part, the results of the soot field investigation will be summarized and discussed, and an approach to rating the sooting tendency of gaseous fuels will be presented.

Soot and Velocity Fields

In turbulent diffusion flames, soot forms in fuel-rich eddies distributed throughout the flame region. Soot is assumed to be formed and contained in these eddies, and its oxidation proceeds through an interaction of soot-containing and oxygen-containing eddies, producing regions containing little or no soot (Magnussen, 1981). The concept of soot-forming eddies and interaction between turbulence and chemical reactions enabled a better understanding of the mechanistism involved in soot formation and oxidation. Consequently, the interaction between the soot and velocity fields is discussed next.

As a matter of illustration, the soot and velocity fields for a propene flame operating at an air/fuel mass ratio of 600 are presented in Figure 6-14. The soot field is characterized by normalized histograms representing soot size and particle number density fluxes. The soot particle fluxes measured in this study are limited to the range of particle sizes resolved by the $60^{o}/20^{o}$ intensity ratioing technique used, thereby excluding the primary particles, which fall into the size range less than 0.08 m. Although the optical measurements do not include the lower limit of the soot size distribution, they do reflect accurately the soot mass loading in the flames.

The maximum soot particle number density flux is observed to be located in the vicinity of the center of the vortex created by the recirculating flow. This location was found to be universal for all the flames studied, and it seems to be a characteristic of the burner. Although this region corresponds to the maximum soot loading, it does not correspond necessarily to the soot-forming region. Soot particles form in fuel-rich eddies and vortices (small structures) shed by the fuel flow jet; the fuel/air equivalence ratio in these eddies is above the threshold or critical equivalence ratio for sooting. The critical equivalence ratio is defined as the ratio of the actual fuel/oxygen ratio divided by the fuel/oxygen ratio needed to burn the fuel completely to carbon dioxide and water vapor.

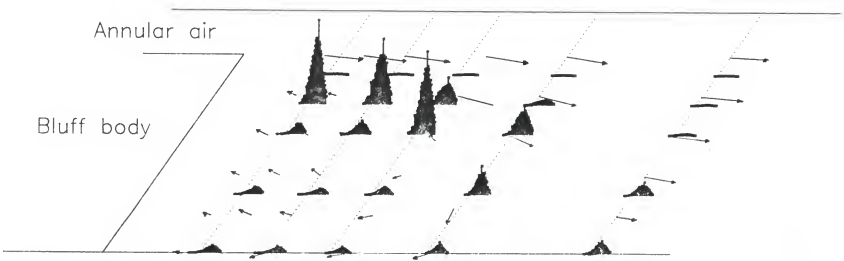

Figure 6-14. Soot and Velocity Fields.

Although combustion may occur throughout the entire region where turbulence is intense, it appears from the temperature data collected for the different flames studied, that the regions where chemical reactions take place are located in the vicinity of the centerline. In this region the recirculated hot products and reactants interact with the fuel jet generating the fuel rich-eddies and the small-scale structures in which chemical reactions take place. The soot precursors are formed inside these eddies, and while they are transported to the center of the vortex where the static pressure is at a minimum, undergo the processes of growth. The soot yield at the exit of the flame is dependent on the turbulence level generated by the interaction of the recirculating flow and the fuel jet. The heat release rate of the fuel, which affects the fuel jet pyrolysis as well as the turbulence generated by the flame, and the fuel structure determine the sooting propensity of a fuel.

A main characteristic of the soot field study is that the soot aggregate sizes were found to be a function solely of the fuel structure rather than of the location of the flames or of the operating conditions. The characteristic soot aggregates found for the different flames were: 0.29 μm for propane flames, 0.31 μm for propene flames, and 0.33 μm for 1-butene and isobutylene flames, respectively.

In the next section soot particle number density will be discussed in relation to the different operating conditions. the soot field mapping is displayed as isoclines (representing soot particle fluxes) deduced from polynomial regression of the data.

Parametric Study of Soot Formation and Oxidation

Fuel flow rate

The effect of fuel flow rate on the sooting field was studied for different flame conditions (Table 6-1). Soot particles leaving the luminous region of the flames studied were measured at a fixed axial locations (x/R = 3). The product of the soot particle number density and the cross-sectional area A_s of the sampling volume perpendicular to the particle velocity are plotted versus the corresponding air/fuel mass ratios in Figures 6-15a, 6-15b, and 6-15c. For all the flames studied, the soot particle number density was found to increase with the fuel flow rate before reaching a maximum at an air/fuel mass ratio of 600, after which a slow decay of the soot particle number density was observed with an increase in the fuel flow rate.

Glassman and Yaccarino (1981) suggested that the increase in the soot yield from diffusion flames derives from an increase in the amount of oxygen from the air side to the reaction zone as the flame is lifted off the burner. This increase in oxygen would eventually serve to accelerate the fuel pyrolysis, which controls soot

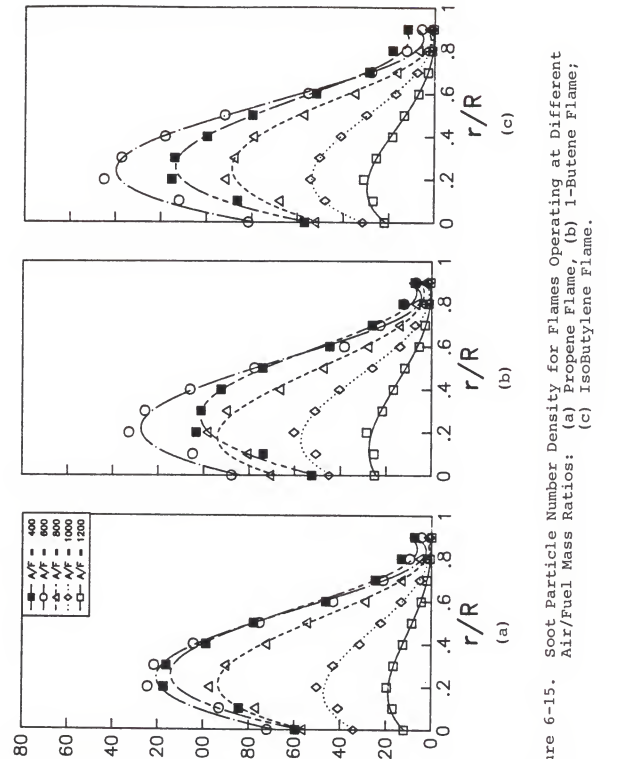

Figure 6-15. Soot Particle Number Density for Flames Operating at Different Air/Fuel Mass Ratios: (a) Propene Flame, (b) 1-Butene Flame; (c) IsoButylene Flame.

formation; however, for this type of burner, an increase in the fuel jet velocity was found to have only a marginal effect on the flow. The maximum temperatures were found in this study to be function of the fuel flow rate and fuel heat content. An increase in the fuel flow rate would increase the number of fuel-rich eddies as well as the number of fine structures in which chemical reactions occur, resulting in higher flame temperatures. These higher temperatures increase the rate of fuel pyrolysis inside the fuel-rich eddies, consequently increasing the concentration of soot precursors as well as the concentration of building blocks such as C_nH_x species necessary for surface growth.

The soot particle number density was observed to reach a maximum before decaying with increasing fuel flow rates. The latter can be explained as follows: an increase in the fuel flow rate results in an increase of the flame temperature that, in turn, increases the rate of fuel pyrolysis and results in higher soot formation rates; however, The increase in the flame temperature with the fuel flow rate affects not only the fuel pyrolysis but also the oxidation rate of the particle. Shug et al. (1980) showed that an increase in the fuel volumetric flow rate increases both the true diffusion flame height and the luminous flame height. The ratio of the height of the luminous zone to the height of the forming zone increases with the fuel flow rate. Consequently the residence time

of the soot particles inside the flame increases with the fuel flow rate. A higher flame temperature in conjunction with a longer residence time of the soot particles results in an increase of the particle oxidation process. Since the soot particles escaping the flame are a function of the competitive processes between the soot particle formation and oxidation, at sufficiently high flow rates the oxidation process dominates the formation process of the particles resulting in lower soot yield.

This trend is confirmed by the results presented in Figures 6-16, 6-17, and 6-18 for the soot fields of propene, 1-butene, and isobutylene flames operating at three air/fuel ratios of 800, 600, and 400. The maximum soot particle flux in the annular region was found to increase with the fuel flow rate. This increase is proportional to the increase in the soot formation rate, henceforth a change in the maximum soot loading in the annular region will be referred as a change in the rate of soot formation. Moreover, an increase in the fuel flow rate was found to increase the soot particle oxidation rate, which was found to increase faster than the rate of soot formation with increasing fuel flow rate. At an air/fuel ratio of 400 the increase in the oxidation rate was observed to dominate the increase in the formation rate of the soot particles.

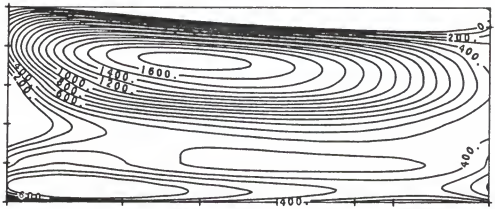

(c)

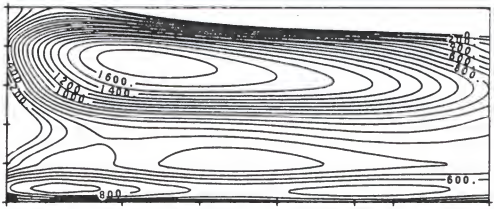

(b)

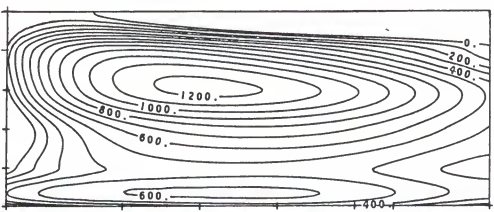

(a)

Figure 6-16. Spatial Mapping of Soot Particle Fluxes for Propene Flames Operating at Different Air/Fuel Ratios: (a) A/F = 800; (b) A/F = 600; (c) A/F = 400.

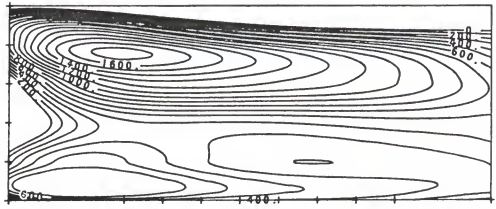

(c)

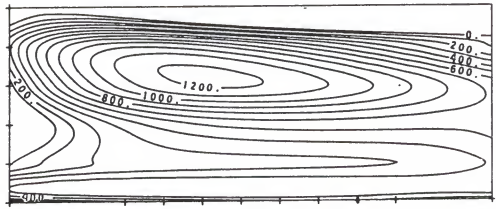

(b)

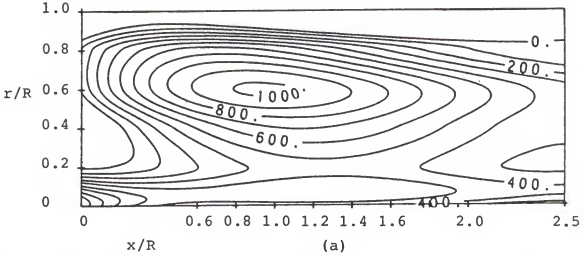

(a)

Figure 6-17. Spatial Mapping of Soot Particle Fluxes for 1-Butene Flames Operating at Different Air/Fuel Mass Ratios: (a) A/F = 800; (b) A/F = 600; (c) A/F = 400.

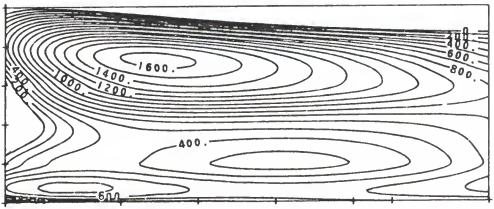

(c)

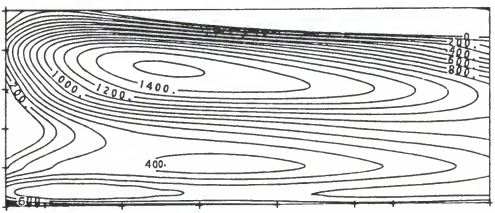

(b)

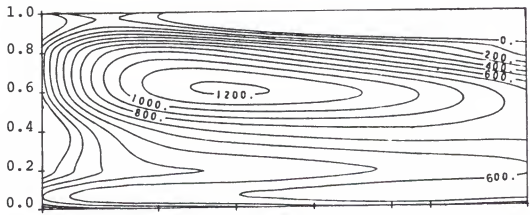

(a)

Figure 6-18. Spatial Mapping of Soot Particle Fluxes for Propene Flames Operating at Different Air/Fuel Ratios: (a) A/F = 800; (b) A/F = 600; (c) A/F = 400.

The results of the product of the total soot particle flux and the cross-sectional area A_s versus air/fuel ratio are presented in Figure 6-19. The total soot particle flux was the integral of the point measurements of soot fluxes over the surface area of the exit plane of the flame. The total soot particle flux, for all the three fuels investigated, increases rapidly with the fuel flow rate (decreasing air/fuel ratios) to reach a maximum at an air/fuel ratio of 600. A further increase of the fuel flow rate shows a slight decrease in the total soot particle flux. The latter shows the competitive aspect of the fuel pyrolysis and soot oxidation. Isobutylene flames were found to soot more than 1-butene, which in turn were found to soot more than Propene. The difference in sooting among the three fueled flames is more prononced at higher fuel flow rates (air/fuel=600). The proposed explanation is that an increase in the fuel flow rate increase both the formation and oxidation of soot particles; however, isobutylene, which is the most sootier of the three fuels studied, produce the lowest flame temperatures at equivalent fuel mass flow rates. thus, the relative increase of the oxidation rate of the soot particles with increasing fuel flow rate is most likely to be lower for low heat content fueled flames.

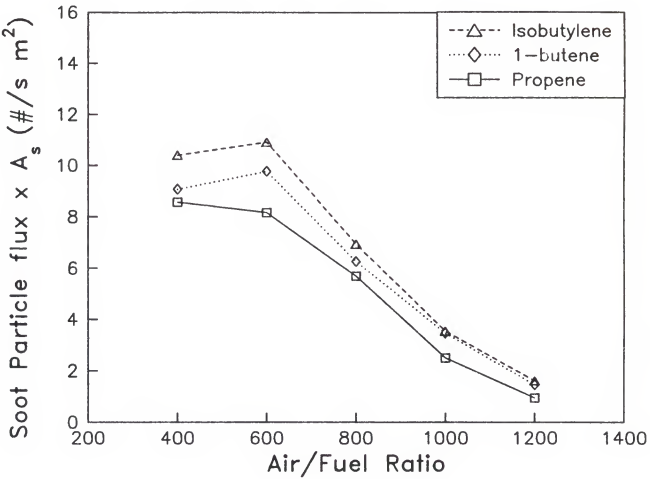

Figure 6-19. Total Soot Particle Yield vs. Air/Fuel Mass Ratios.

Fuel stream heat content

Both the fuel jet velocity and the potential fuel stream heat content were thought to affect the temperature and the soot fields. This set of experiments (Table 6-2) was designed to separate the effect of fuel jet velocity from the effects of heat release rate on soot production. The fuel jet velocities were kept constant by progressively replacing nitrogen by fuel. Consequently the fuel stream heat content was varied while the fuel jet velocity was maintained constant.

The results for this set of experiments are presented in Figures 6-20a, 6-20b, and 6-20c for propene, 1-butene, and isobutylene flames, respectively. Similar to the results of Experiment I, The soot particle number density exiting from the flame was found to increase, reach a maximum, and decay as the fuel flow rate was increased. The flame temperatures were observed to increase and the number of fuel-rich eddies was presumably increased with the fuel flow rate. Thus, both the rate of pyrolysis of the fuel and oxidation of the soot particles were affected by the increase in the fuel flow rate.

Soot field data are presented in Figures 6-21, 6-22, and 6-23 for a selected set of operating conditions of Experiment II. These results show that an increase in the fuel mass flow rate resulted in an increase of both the amount of the soot formed and the rate of oxidation of these particles. The rate of oxidation was observed to

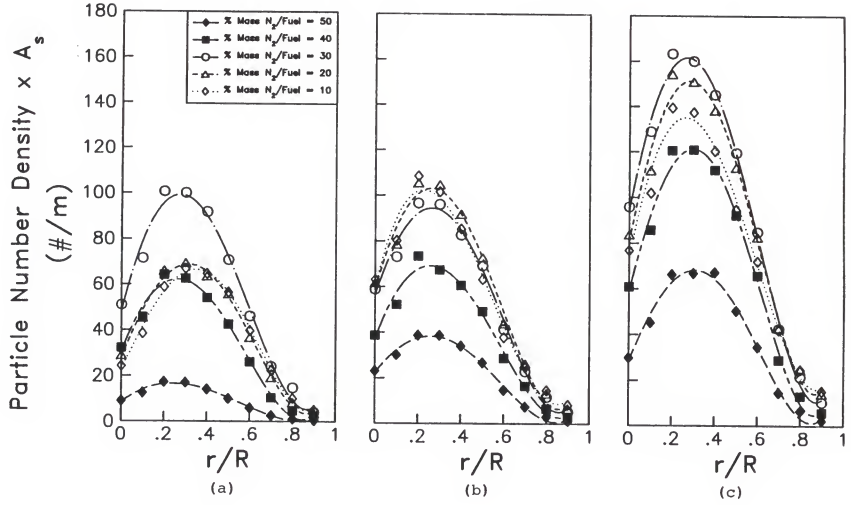

Figure 6-20. Soot Particle Number Density for Flames Operating at Different Nitrogen/Fuel Gas Mixture Ratios: (a) Propene; (b) 1-Butene (c) Isobutylene

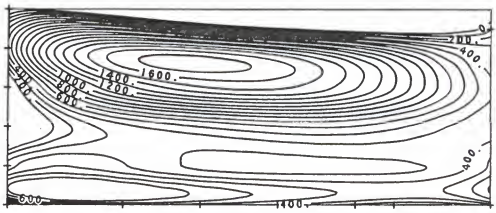

(c)

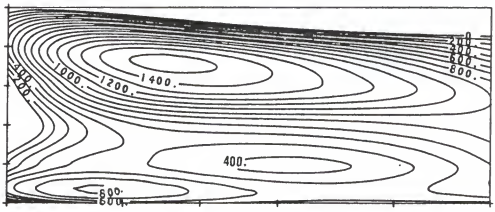

(b)

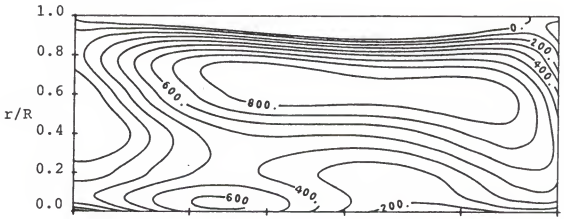

(a)

Figure 6-21. Spatial Mapping of Soot Particle Fluxes for Propene Flames Operating at Different Air/Fuel Mass Ratios: Nitrogen/Fuel Mass Flow Rate Constant: (a) A/F = 800; (b) A/F = 600; (c) A/F = 400.

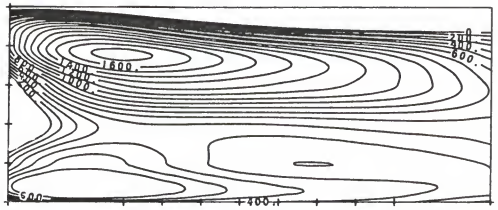

(c)

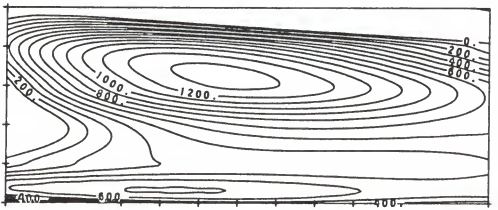

(b)

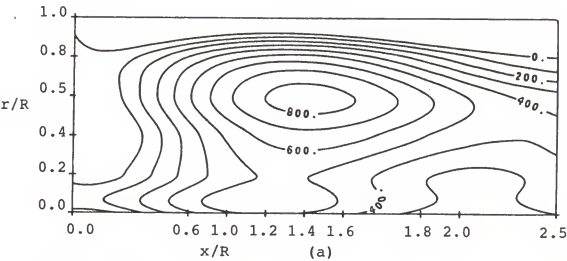

(a)

Figure 6-22. Spatial Mapping of Soot Particle Fluxes for 1-Butene Flames Operating at Different Air/Fuel Ratios: Nitrogen/Fuel Mass Flow Rates Constant: (a) A/F = 800, (b) A/F = 600; (c) A/F = 400.

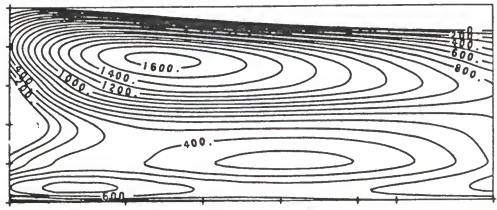

(c)

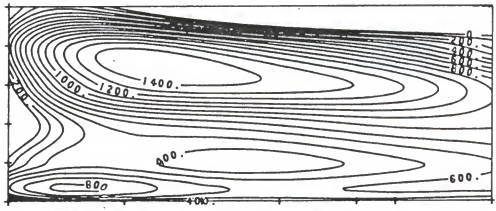

(b)

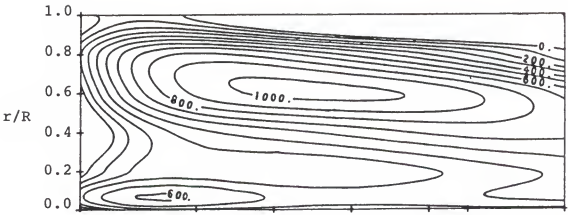

(a)

Figure 6-23. Spatial Mapping of Soot Particle Fluxes for Isobutylene Flames Operating at Different Air/Fuel Ratios: Nitrogen/Fuel Mass Flow Rates Constant: (a) A/F = 800; (b) A/F = 600; (c) A/F = 400.

increase faster than the rate of formation as the fuel flow rate increased for this set of experiments. The fuel stream heat content appears to be the principal parameter that determines the fate of a soot particle.

The total soot particle flux versus the mass ratio of fuel and nitrogen is displayed in Figure 6-24. As discussed above, the total soot particle flux is shown to to reach a maximum before decreasing slowly with increasing fuel/nitrogen mass ratios. Nitrogen dilution reveal a more prononced effect on the relative sooting tendency of different fuels. The difference in sooting rates among the three fuels studied was found to be larger in the presence of nitrogen. Isobutylene which has the lower heat content was found to soot more readily than the two other fuels investgated. A priori, for this type of burner configuration, nitrogen dilution has a more profond effect on the oxidation rate of the soot particles when using fuels with lower heat content.

Nitrogen dilution

This set of experiments (Table 6-3) was set up to determine nitrogen dilution effect for constant fuel stream heat content. Nitrogen was added gradually to a constant mass flow rate of fuel. The results relating the soot yield to the volumetric flow rate of added nitrogen are presented in Figures 6-25a, 6-25b, and 6-25c for propene, 1-butene, and isobutylene flames, respectively, operating at a constant fuel stream heat content of 196 Btu/min., An

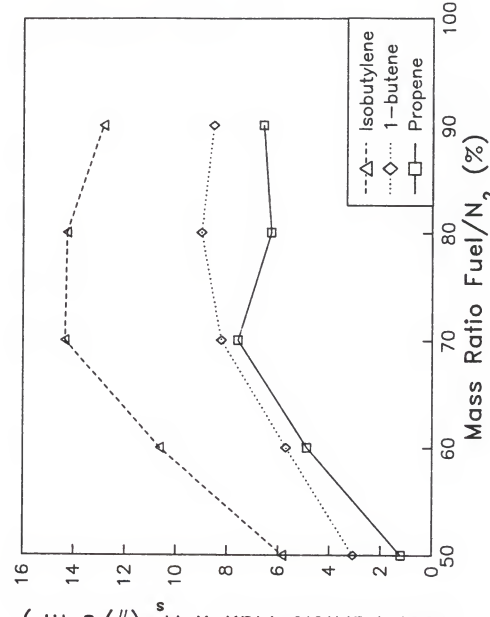

Figure 6-24. Total Soot Particle Yield vs. Fuel/N_2 Mass Ratios.

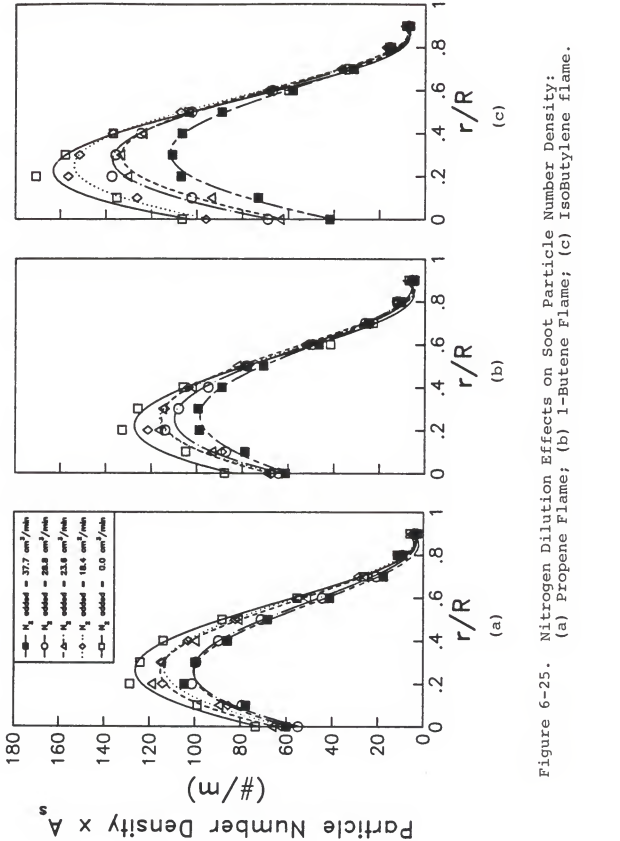

Figure 6-25. Nitrogen Dilution Effects on Soot Particle Number Density: (a) Propene Flame; (b) 1-Butene Flame; (c) IsoButylene Flame.

increase in the nitrogen flow rate was found to decrease slightly the amount of soot emitted. Temperature measurements showed no significant change with nitrogen dilution. Further, Shug et al. (1980) found that nitrogen dilution had no effect on the luminous flame height. Therefore the soot oxidation rate should not be greatly affected by nitrogen dilution. the slight decrease observed in the soot emission with the fuel jet velocity could be the result of a lean out of the fuel rich eddies by Nitrogen dilution.

The soot mapping of a series of flames from Experiment III are presented in Figures 6-26, 6-27, and 6-28 for propene, 1-butene, and isobutylene flames, respectively. Indeed, an increase in the nitrogen flow rate was found to decrease the amount of soot formed in the annular region of the flames. An exception to this trend was observed for a 1-Butene flame (Flame III9). This is due to a slightly higher fuel flow rate for this flame as compared to the other two flame conditions. The decrease in the amount of soot formed in the annular region should be attributed to a decrease in the fuel pyrolysis which is temperature dependent; however, temperature measurements showed no significant change with nitrogen dilution. The probable explanation is that the reaction and soot forming regions are too thin to measure their local temperatures, and that the measured temperature are averaged temperatures. Consequently, a decrease in temperature in

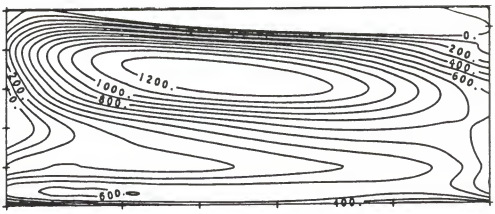

(c)

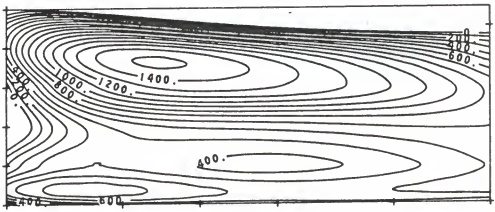

(b)

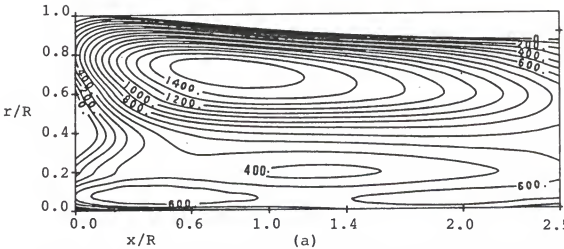

(a)

Figure 6-26. Spatial Mapping of Soot Particle Fluxes for Propene Flames: Nitrogen Dilution Effects (Nitrogen Added: (a) 18.4 cm^3/s; (b) 23.6 cm^3/s; (c) 28.8 cm^3/s).

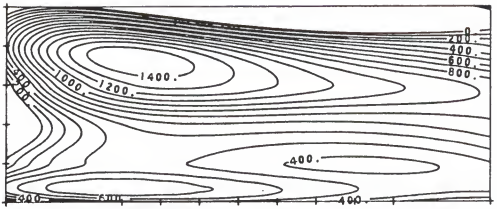

(c)

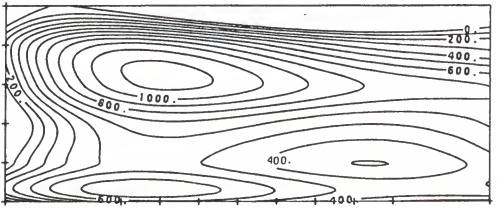

(b)

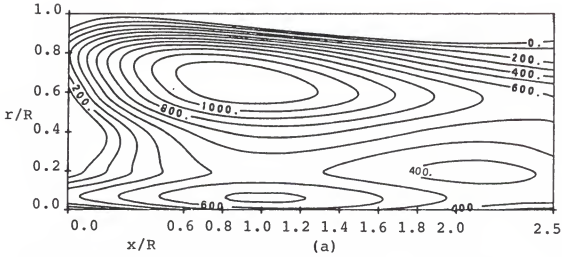

(a)

Figure 6-27. Spatial Mapping of Soot Particle Fluxes for 1-Butene Flames: Nitrogen Dilution Effects (Nitrogen Added: (a) 18.4 cm^3/s; (b) 23.6 cm^3/s; (c) 28.8 cm^3/s.

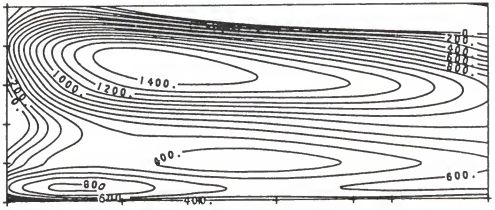

(c)

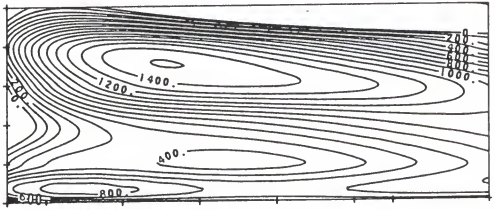

(b)

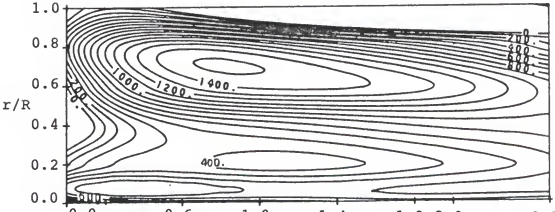

(a)

Figure 6-28. Spatial Mapping of Soot Particle Fluxes for Isobutylene Flames: Nitrogen Dilution Effects: Sitrogen Added: (a) 18.4 cm^3/s; (b) 23.6 cm^3/s; (c) 28.8 cm^3/s.

the reaction and soot-forming regions could not be detected by the thermocouples used. The hypothesis is that nitrogen dilution in the the fuel-rich eddies would compete for the energy released from the chemical reactions reducing the fuel pyrolysis. The total soot particle flux emitted from the flames is shown to decrease linearly with increasing nitrogen volumetric flow rate (Figure 6-29).

Air reference velocity

The air velocity was found to be the main parameter that control the aerodynamics of the flames for these kind of burners. The luminous length of the flames seemed to shrink slightly and the flame temperatures cooler as the the air jet velocity was increased. The effect of the air velocity on the soot escaping at the flame front was studied for different flame where the fuel type and air -velocity were varied while the fuel jet velocity was kept constant (Experiment IV).

The results for these experiments are shown in Figures 6-30a, 6-30b, and 6-30c for propene, 1-butene, and isobutylene flames, respectively. The amount of soot emitted from the flames was observed to decrease as the air velocity was increased. The question that had to be answered is why less soot was emitted although the oxidation rate of the formed soot particles should have decreased because of the reasons cited above ?.

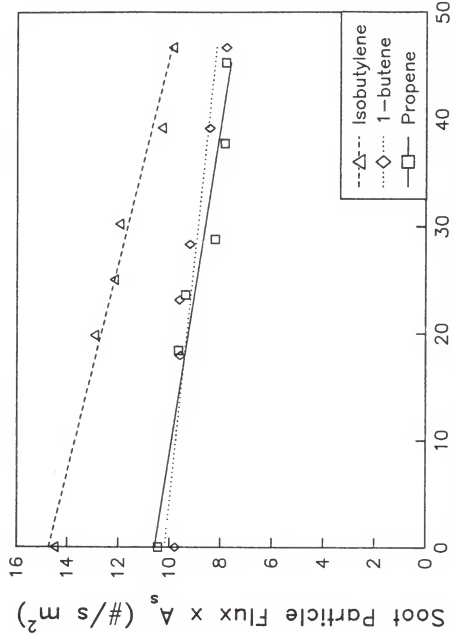

Figure 6-29. Total Soot Particle Yield vs. Volumetric Flow Rate of N_2 Added.

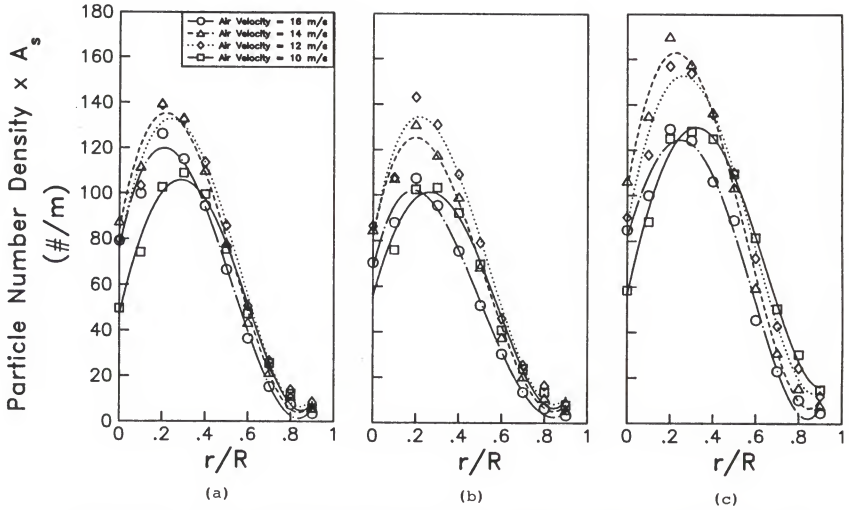

Figure 6-30. Air Reference Velocity Effects on Soot Particle Number Density: (a) Propene Flame; (b) 1-Butene Flame (c) IsoButylene Flame.

To answer this question, the soot mapping of these flames was performed. The results are presented in Figures 6-31, 6-32, and 6-33 for propene, 1-butene, and isobutylene flames. The soot particle concentration in the annular region of the flame was observed to decrease and their oxidation rate to increase with the air velocity. The decrease in the soot particle formation could have been the result of a decrease in the fuel rich eddies because of better mixing and leaner environment. Therefore, lesser soot particle inside the flames could have resulted in higher oxidation energy available for each specific particle. The latter could explain the increase in the particle oxidation rate although the flames appeared cooler when the air jet velocity was increased. The total soot particle flux is is shown to decrease slightly with the air reference velocity (Figure 6-34)

Discussion

The heat release rate was observed to be the dominant parameter controlling the competitive processes of pyrolysis of the fuel and oxidation of soot particles; however, consideration of the heat content of each fuel studied reveals that isobutylene, which has the lower heat content, was the most-prolific sooting fuel. Thus, the fuel stream heat content alone does not define the sooting tendency of a fuel; nonetheless, it is an important parameter that can be used, together with the fuel

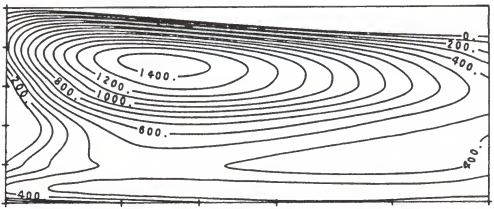

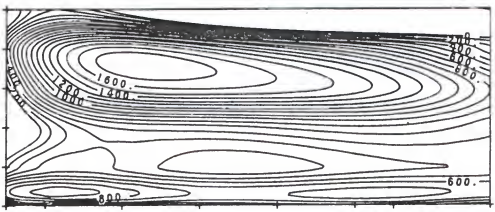

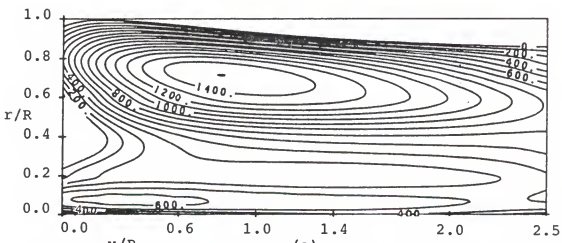

Figure 6-31. Spatial Mapping of Soot Particle Fluxes for Propene Flames Operating at Different Air Reference Velocities: (a) 12 m/s; (b) 14 m/s; (c) 16 m/s.

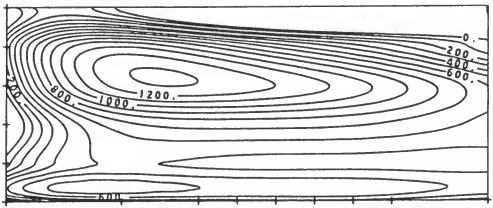

(c)

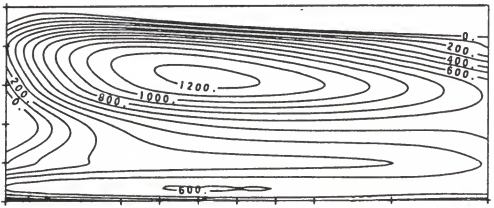

(b)

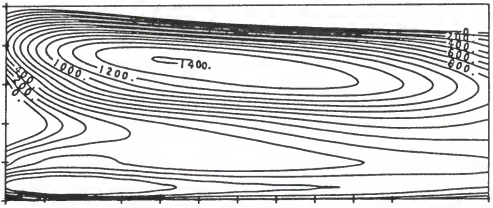

1.0
0.8
0.6
r/X
0.4
0.2
0.0

0.0 0.6 0.8 1.0 1.2 1.4 1.6 1.8 2.0 2.5

x/R

(a)

Figure 6-32. Spatial Mapping of Soot Particle Fluxes for 1-Butene Flames Operating at Different Air Reference Velocities: (a) 12 m/s; (b) 14 m/s; (c) 16 m/s.

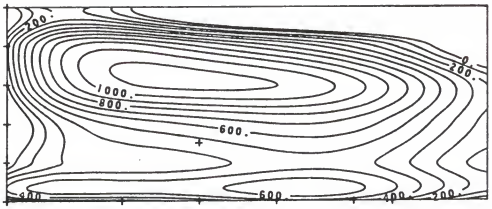

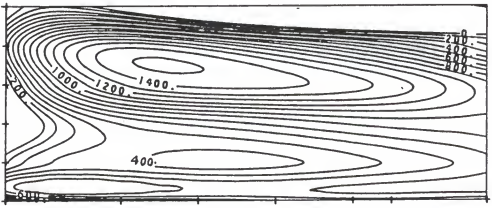

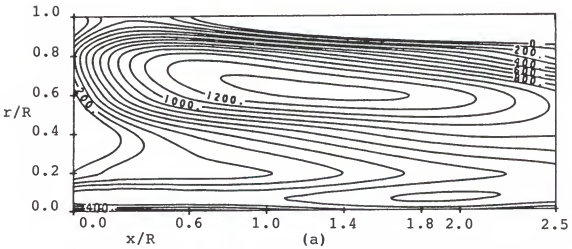

Figure 6-33. Spatial Mapping of Soot Particle Count Rates for Isobutylene Flames Operating at Different Air Reference Velocities: (a) 12 m/s; (b) 14 m/s; (c) 16 m/s.

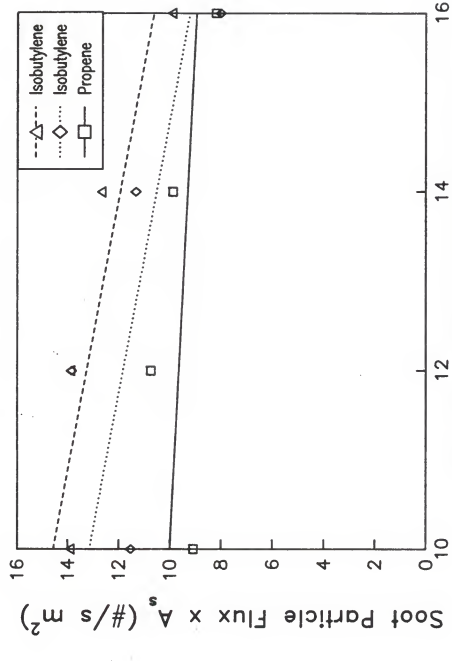

Figure 6-34. Total Soot Particle Yield vs. Air Reference Velocity.

structure, to estimate the propensity of fuels to soot in turbulent diffusion flames.

Glassman and Yaccarino (1981) postulated that the rate of fuel pyrolysis determines the degree of sooting. Since the rate of fuel pyrolysis is temperature-dependent, they proposed a temperature-correlation method, based on calculated adiabatic temperatures (T), to determine the sooting tendency of different fuels. Assuming that the pyrolysis reaction follows Arrhenius kinetics, they concluded that the reciprocal of the logarithm of the fuel flow rate corresponding to the onset of sooting versus (1/T) should produce straight lines for each fuel. The results of their experiments effectively reveal a linear relationship between the logarithm of the fuel mass flow rate and the inverse of the adiabatic temperatures.

The type of flames investigated in this study are highly turbulent and recirculating. The high-intensity turbulence associated with these flames does not allow combustion to be limited to a well defined, thin reaction zone. Instead, the chemical reactions, as mentioned earlier, occur in localized regions associated with the turbulence. Because of the recirculation associated with bluff-body burners, the sooting height, used by Glassman and Yaccarino (1981) to determine the onset of sooting of different fuels, can not be used in these circumstances to determine the tendency of fuel to soot. Further, the use of calculated adiabatic temperatures to correlate the

sooting tendency of fuels may not reflect the actual temperatures in the flames. The flame temperatures are lower than the corresponding adiabatic temperatures due to radiation from the soot particles, incomplete combustion, and convection losses from the flames to the cool air stream.

An alternative parameter to correlate the sooting tendency of different fuels in highly turbulent flames is the potential heat of the fuel stream. Although this parameter is directly related to the calculated adiabatic temperature, its advantage over the latter in rating the soot propensity to soot is in its availability for use without complex computations of adiabatic temperatures. Moreover, the potential heat of the fuel stream is an accessible controlling parameter.

The potential heat of the fuel stream was found in this study to be the main parameter that determines the fate of a soot particle. This parameter was found to have a direct effect on the competitive processes of formation and oxidation of the soot particles. A plot of the total emitted soot particle flux versus the potential fuel heat content is shown in Figure 6-35. The sooting rate is shown to increase with the potential heat content of the fuel stream before reaching a maximum. Isobutylene is shown to be the sootiest followed by 1-butene and propene. This sooting order agrees with the data of Glassman and Yaccarino (1981).

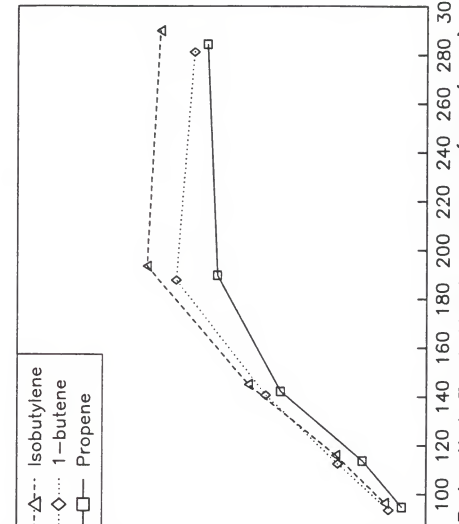

Figure 6-35. Total Soot Particle Flux vs. Potential Fuel Stream Heat Content.

CHAPTER VII
CONCLUSIONS AND RECOMMENDATIONS

Conclusions

The present study is an investigation of the effect of fuel type, fuel stream heat content, nitrogen dilution, and air jet velocity on the respective rates of formation burnout of soot particles in a highly recirculating, turbulent-type flame. Notwithstanding the appreciable support of physical probes for data collection in such areas as temperature measurements, gas sampling and particle sampling, this study stressed the use of a nonintrusive optical technique (IPSS) to measure particle size distribution and flux of soot particles behind a bluff-body burner.

The conclusions that have been drawn from these experiments are summarized as follows:

1. The performance of the Integrated Particle Sizing System (IPSS) as a viable non-intrusive optical instrument for measuring the size and count rate of particles has been demonstrated in this study for both non-reacting and reacting flows. This instrument was found particularly useful in this study because it does not interfere with the chemical and physical processes occurring in flames.

2. Chemical analysis of the composition of the PAHs extracted from soot samples collected at the face of the burner and on a filter located downstream in the exhaust system suggests the operation of multiple, convergent pathways rather than one chemical mechanism leading to the formation of high molecular weight PAHs and soot.

3. A fuel's relative tendency to soot is a measure of relative rates of competitive processes of pyrolysis of fuel and of burnout of the soot particles. The experimental results of this study aggree with the reported literature that flame temperature distribution and type of fuel burned are the dominant parameters that determine the relative importance of fuel pyrolysis and soot particle oxidation in highly turbulent recirculating flames.

4. The potential fuel stream is presented in this study as a usefull correlating parameter to evaluate the propensity of a fuel to soot in turbulent flames.

5. The differences in sooting rates among the fuels studied were found to be larger in the presence of nitrogen. The rate of oxidation of soot particles in flames burning low-heat content fuels exhibit greater sensitivity to addition of nitrogen. Lower overall flame temperatures decrease the burnout of the soot particles.

Recommendations

An improvement of the accuracy of the optical system can be realized through a probe volume correction that would takes into account the effects of the intensity variation of the laser beam in the sampling space and the scattering characteristics of the particle to be measured.

More experiments using different burner configurations will be needed to assert the usefullness of the potential fuel stream heat content to correlate the sooting tendencies of different fuels.

The experimental results from this study will provide insights into the complex field of soot formation and burnout. The soot particle path, flowfield, and temperature distribution inside the flames will provide information for modeling studies. Further, characterization of the main parameters that affect net soot production can be used to determine the propensity of a fuel to soot.

REFERENCES

Appleton, J.P., "Soot Oxidation Kinetics at Combustion Temperature," in Atmospheric Pollution by Aircraft Engines AGARD, paper 20, 1973.

Becker, H.A., Yamazaki, S., "Soot Concentration Field of Turbulent Propane/Air Diffusion Flames," 16th Symposium (Int.) on Combustion, the Combustion Institute, Pittsburgh, p.681, 1977.

Bittner, J.D., and Howard, J.B., "Composition Profiles and and Reaction Mechanisms in a Near Sooting Benzene Oxygen/Argon Flame, "18th Symposium (Int.) on Combustion, the Combustion Institute, Pittsburgh, p.1105, 1981a.

Bittner, J.D., and Howard, J.B., "Pre-particle Chemistry in Soot Formation" in Particulate Carbon Formation During Combustion (Siegla, D.C., Smith, G.W., ed.), Plenum Press, New York, p.109, 1981b.

Blyholder, G., Binford, J.S., and Eyring, H., "A Kinetic Theory for the Oxidation of Carbonized Filaments," J. Phys. Chem. 62, p.263, 1958.

Bonne, U., Homann, K.H., and Wagner, H.G., "Carbon Formation in Premixed Flames," 10th Symposium (Int.) on Combustion, the Combustion Institute, Pittsburgh, p.503, 1965.

Brill, F.W., and Eyler, J.R., "Sequential Ion-molecule reactions in Acetylene," J. Phys. Chem. 85, p.1091, 1981.

Calcote, H.F., "Ion Production and Recombination in Flames," 8th Symposium (Int.) on Combustion, Williams and Wilkins Co., Baltimore, p.184, 1962.

Calcote, H.F., "Ion and Electron Profiles in Flames," 9th Symposium (Int.) on Combustion, The Combustion Institute, Pittsburgh, p.622, 1963.

Calcote, H.F., "Mechanisms of Soot Nucleation in Flames," Combustion and Flames 42, p.215, 1981.

Calcote, H.F., and Manos, D.M., "Effect of Molecular Structure on Incipient Soot Formation," Combustion and Flames 49, p.289, 1983.

Chul P., and Appleton, J.P., "Shock-Tube Measurements of Soot Oxidation Rates," Combustion and Flames 20, p.369, 1973.

Crittenden, B.D., and Long, R.,"Formation of Polycyclic Aromatic in Premixed Acetylene and Ethylene Flames," Combustion and Flame 20, p.359, 1973.

Cullis, C.F., Read, I.A., and Trimm, D.L., "The Role of Acetylenic Hydrocarbons on the Formation of Carbon From Gases," 11th Symposium (Int.) on Combustion, the Combustion Institute, Pittsburgh, p.391, 1967.

D´Alessio, A., Di-Lorenzo, A., Borghese., A., Beretta, F., and Massi S., "Study of the Soot Nucleation Zone of Rich Methane-Oxygen Flames," 16th Symposium (Int.) on Combustion, the Combustion Institute, Pittsburgh, p.695, 1977.

Dave, J. V., "Subroutines for Computing the Parameters of the Electromagnetic Radiation Scattred by a Sphere," IBM 320-3237, IBM Corp., Palo Alto, California, 1968.

DiLorenzo, A., D´Alessio, A., Cincotti, V., Massi, S., Menna, P., and Venitozzi, C., "U.V. Absorption, Laser Excited Fluorescence, and Direct sampling in the study of P.A.H. in rich $CH4/O_2$ Flames," 18th Symposium (Int.) on Combustion, The Combustion Institute, Pittsburgh, p.485, 1981.

Dyer, T.M., and Flower, W.L., "A Phenomenological Description of Particulate Formation During Constant Volume Combustion," in Particulate Carbon Formation During Combustion (Siegla, D.C., Smith, G.W., ed.), Plenum Press, New-York, 1981.

Edelman, R.B., and Fortune, O.F., "A Quasi-Global Chemical Kinetic Model for the Finite-Rate Combustion of Hydrocarbon Fuels With Application to Turbulent Burning and Mixing in Hypersonic Engines and Nozzles," AIAA, p.69, 1969.

Edelman, R.B., Turan, A., Harsha, P.T., Wong, E., and Blazowski, W.S., "Fundamental Characterization of Alternative Fuel Effects in Combustion Systems," paper 13, AGARD-CP-275, 1979.

Edelman, R.B., Farmer, R.C., and Wang, T.S., "Combustion and Emission of Synthetic Fuel Components, Analysis and Modeling," (Bartok, W., ed.), American Chemical Society Symposium Series, Washington, D.C., p.29, 1983.

Eyler, J.R., "Reactivities and Structure of Some Hydrocarbon Ions and their Relationship to Soot Formation," in The Chemistry of Combustion Processes (Sloane, T.M., ed.), American Chemical Society Symposium Series, Washington, D.C., p.49., 1984.

Farmer, R., Edelman, R.B., and Wong, E., "Modeling Soot Emissions in Combustion System," in Particular Carbon During Combustion (Siegla, D.C., and Smith, G.W., ed.), Plenum Press, New-York, p.299, 1981.

Frenklach, M., Taki, S., and Matula, R.A., "LDV Measurement of Soot Particle Size," 1982 Technical Meeting, the Eastern Section of the Combustion Institute, New Jersey, paper 16, 1982.

Frenklach, M., Taki, S., and Matula, R.A., "A Conceptual Model for Soot Formation in Pyrolysis of Aromatic Hydrocarbons," Combustion and Flame 49, p.275, 1983a.

Frenklach, M., Taki, S., Durgaprasad, M.B., and Matula, R.A., "Soot Formation in Pyrolysis of Acetylene, Allene and 1-3 butadiene," 1983 Spring Technical Meeting, Western Section of the Combustion Institute, Pasadena, California, 1983b.

Galant, S., Grousset, D., Martinez, G., and Micheau, P., "Three-dimensional Steady Parabolic Calculations of Large Scale Methane Diffusion Flames to Predict Flare Radiation Under Cross-Wind Conditions," 20th Symposium (Int.) on Combustion, the Combustion Institute, Pittsburgh, p.531, 1984.

Gaydon, A.G., and Wolfhard, H.G., Flames, Third Edition, Chapman and Hall, London, 1970.

Glassman, I., "Phenomenological Models of Soot Processes in Combustion System," Dept. of Mech. and Aerospace Eng., Report 1450, Princeton University, 1979.

Glassman, I., and Yaccarino, P., "The Temperature Effect in Sooting Diffusion Flames," 18th Symposium (Int.) on Combustion, the Combustion Institute, Pittsburgh, p.1175, 1981.

Gomez, A., Sidebotham, G., and Glassman, I., "Sooting Behavior in Temperature-Controlled Laminar Diffusion Flames," Combustion and Flame 58, p.58, 1984.

Goodings, J.M., Bohme, D.K., and Chung-Waing, "Detailed Ion Chemistry in Methane-Oxygen Flames, I. Positive Ions," Combustion and Flame 36, p.27, 1979a.

Goodings, J.M., Bohme, D.V., and Chung-Waing, "Detailed Ion Chemisty in Methane-Oxygen Flames, II. Negative Ions," Combustion and Flame 36, p.44, 1979b.

Graham, S.C., "The Collisional Growth of Soot Particles at High Temperatures," 16th Symposium (Int.) on Combustion, the Combustion Institute, Pittsburgh, p.663, 1977.

Graham, S.C., "The Modeling of the Growth of Soot Particles During The Pyrolysis and Partial Oxidation of Aromatic Hydrocarbons," Proc. Roy. Soc., London, A377, p.119, 1981.

Hack, R.L., Samuelsen, G.S., Poon, C.C., and Bachalo, W.D., "An Exploratory Study of Soot Sample Integrity and Probe Perturbation in a Swirl-Stabilized Combustor," J. of Eng. for Power, 103, p.759, 1981.

Harris, S.J., "Surface Growth of Soot in Premixed Flames," in Chemical and Processes in Combustion, 1982 Technical Meeting, the Eastern Section of the Combustion Institute, New-Jersey, Paper 27, 1982.

Haynes, B.S., Jander, H., and Wagner, H.G., "The Effect of Metal Additives on the Formation of Soot in Premixed Flames," 18th Symposium (Int.) on Combustion, the Combustion Institute, Pittsburgh, p.1365, 1981.

Homann, K.H., and Wagner, H.G., "Some New Aspects of the Mechanism of Carbon Formation in Premixed Flames," 11th Symposium (Int.) on Combustion, the Combustion Institute, Pittsburgh, p.371, 1967.

Homann, K.H., and Wagner, H.G., "Chemistry of Carbon Formation in Flames," Proc. Roy. Soc. London, A307 p.141, 1968.

Hurle, I.R., Sugden, T.M., and Nutt, G.B., "Chemi-Ionization of Nitric-Oxide in Flames Containing Hydrocarbons Additives", 12th Symposium (Int.) on Combustion, the Combustion Institute, Pittsburgh, p.387, 1969.

Jensen, D.E., "Predictions of Soot Formation Rates: A New Approach," Proc. Roy. Soc., London, A338, p.375. 1974.

Kent, J.H., Jander, H., and Wagner, H.Gg., "Soot Formation in Laminar Diffusion Flames," 18th Symposium (Int.) on Combustion, the Combustion Institute, Pittsburgh, p.1117, 1981.

Kent, J.H., and Wagner, H.Gg, "Soot Measurements in Laminar Ethylene Diffuson Flames," Combustion and Flame 47, p.53, 1982.

Kerker, M., The Scattering of Light and other Electromagnetic Radiations, Academic Press, New-York, 1969.

Khan, I.M., and Greeves, G., "A Method for Calculating the Formation and Combustion of Soot on Diesel Engines," in Heat Transfer in Flames, (Afgan, N.H., and Beer, J.M., ed.), Chapter Press, New-York, p.285, 1974.

Kinbara, T., and Noda, K., "Ion Formation in the Photochemically Initiated Combustion of C_2H_2-O_2-NO_2 Mixtures: Part II. Ion Current and Emission Spectra, "13th Symposium (Int.) on Combustion, the Combustion Institute, Pittsburgh, p.333, 1971.

Kinbara, T., and Noda, K., "Relation between Ion Creation and C_2, CH and OH Formation in the Combustion of Hydrocarbons," 14th Symposium (Int.) on Combustion, the Combustion Institute, Pittsburgh, p.321, 1973.

Knewstubb, P.F., and Sugden, T.M., "Mass Spectrometry of the Ions Present in Hydrocarbon Flames," 7th Symposium (Int.) on Combustion, Butterworths, London, p.247, 1959.

Kowalik, R.M., Ruth, L.A., and Blazowski, W.S., "Soot Formation in a Jet Stirred Reactor," in Particulate Carbon Formation During Combustion (Siegla, D.C., and Smith, G.W., ed.), Plenum Press, New-York, p.285, 1981.

Lee, B.B., Thring, M.W., and Beer, J.M., "On the Rate of Combustion of soot in a laminar flame," Combustion and Flame 6, p.137, 1962.

Magnussen, B.F., "Modeling of Reaction Processes in Turbulent Flames with Special Emphasis on Soot Formation and Combustion," in Particulate Formation During Combustion (Siegla, D.C., and Smith, G.W., Ed.), Plenum Press, New-York, p.321, 1981.

Magnussen, B.F., Hjertager, B.H., Olsen, J.G., and Bhaduri, D., "Effects of Turbulent Structure and Local Concentrations on Soot Formation and Combustion in C_2H_2 Diffusion Flames," 16th Symposium (Int.) on Combustion, the Combustion Intitute, Pittsburgh, p.719, 1977.

Michaud, P., Delfaud, J.L., and Barassin, A., "The Positive Ion Chemistry in the Post-Combustion Zone of Sooting Premixed Acetylene Low Pressure Flat Flames," 18th Symposium (Int.) on Combustion, the Combustion Institute, Pittsburgh, p.443, 1981.

Millikan, R. C., "Non-Equilibrium Soot Formation in Premixed Flames," J. Phys. Chem. 66, p.794, 1962.

Miller, W.J., "Ions in Flames," 14th Symposium (Int.) on Combustion, the Combustion Institute, Pittsburgh, p.307, 1973.

Nagle, J., and Strickland-Constable, R.F., "Oxidation of Carbon Between 1000-2000^{o}C," Proc. Fifth Carbon Conf. 1, p.154, 1962.

Neoh, K.G., Howard, J.B., and Sarofim, A.F., "Soot Oxidation in Flames," in Particulate Carbon Formation During Combustion (Siegla, D.C., and Smith, G.W., ed.), Plenum Press, New-York, p.261, 1981.

Nishida O., and Mukohara S., "Characteristics of Soot Formation and Decomposition in Turbulent Diffusion Flames," Combustion and Flame 47, p.269, 1982.

Olson, D.B. and Calcote, H.F., "Ionic Mechanisms of Soot Nucleation in Premixed Flames," in Particulate Carbon Formation During Combustion (D.C. Siegla and G.W. Smith ed.), Plenum Press, New-York, p.177, 1981a.

Olson, D.B., and Calcote, H.F., "Ions in Fuel-Rich and Sooting Acetylene and Benzene Flames," "18th Symposium (Int.) on Combustion, the Combustion Institute, Pittsburg, p.453, 1981b.

Palmer, H.B., and Cullis, C.F., "The Formation of Carbon from Gases", in Chemistry and Physics of Carbon (Walker, P.L., ed.), Marcel Dekker, Inc., New-York, p.265, 1965.

Peeters, J., and Van Tiggelin, A., "Experimental Determination of the Rate of the Chemi-ionization Process", 12th Symposium (Int.) on Combustion, the Combustion Institute, Pittsburgh, p.437, 1969.

Prado, G.P., Lee, M.L., Hites, R.A., Hoult, D.P., and Howard, J.B., "Soot and Hydrocarbons Formation in a Turbulent Diffusion Flame," 16th Symposium (Int.) on Combustion, the Combustion Institute Pittsburgh, p.649, 1977.

Prado, G.P., Jagoda, J., Neoh, K., and Lahaye, J., "A Study of Soot Formation in Premixed Propane/Oxygen Flame by In-Situ Optical Techniques and Sampling Probes," 18th Symposium (Int.) on Combustion, the Combustion Institute, Pittsburgh, p.127, 1981.

Prado, G.P., and Lahaye, J., "Physical Aspects of Nucleation and Growth of Soot Particles," in Particulate Carbon Formation During Combustion (Sigla, D.C., and Smith, G.W., ed.), Plenum Press, New-York, p.143, 1981.

Radcliffe, S.W., and Appleton, J.P., "Shock-Tube Measurements of Carbon to Oxygen Atom Ratios for Incipient Soot Formation with C_2H_2, C_2H_4 and C_2H_6 Fuels," Combustion Science and Technology 3, p.255, 1971.

Rawlins, W.T., Schertzer, S.P., and Tanzawa, T., "Observation of Soot Initiation in the Pyrolysis and Combustion of Toluene," 1982 Technical Meeting, the Eastern Section of the Combustion Institute, New-Jersey, paper 29, 1982.

Roe, L.A., Investigation of the Flowfield in a Centerbody Diffusion Burner Using a Laser Doppler Anemometer, Phd. Dissertation, Mech. Eng. Dept., Univ. of Florida, Gainesville, Fl., 1987.

Roquemore, W.M., Bradley, R.P., Stutrud, J.S., Reeves, C.M., Obringer, C.A., and Britton, R.L., "Utilization of Laser Diagnostics to Evaluate Combustor Models," Combustion Problems in Turbine Engines, AGARD CP-333, 19, p.1151, 1983.

Santoro, R.J., and Semerjian, H.G., and Dobbins, R.A., "Soot Particles Measurements in Diffusion Flames," Combustion and Flame 51, p.208, 1983.

Santoro, R.J., and Semerjian, H.G., "Soot Formation in Diffusion Flames: Effects of Fuel Structure, Temperature and Pressure," AFOSR No. AFOSR ISSA85-0025, 1985.

Shug, K.P., Manheimer-Timnat, Y., Yaccarino, P., and Glassman, I., "Sooting Behavior of Gaseous Hydrocarbon Diffusion Flames and the Influence of Hydrocarbons," Combustion Science and Technology 22, p.235, 1980.

Smyth, K.C., and Mallard, W.G., "Laser Induced Ionization and Mobility Measurements of Very Small Particles in Premixed Flames at the Sooting Limit," Combustion Science and Technology 26, p.35, 1981.

Smyth, K.C., Lias, S.G., and Ausloos, P., "The Ion-Molecule Chemistry of $C_3H_3^+$ and the Implications for Soot Formation," Combustion Science and Technology 28, p.147, 1982.

Stein, S.E., "ON the High Temperature Chemical Equilibria of Polycyclic Aromatic Hydrocarbons," J. of Phy. Chem. 82, p.566, 1978.

Stein, S.E., "Structure and Equilibria of Polycyclic Aromatic Flame Ions," Combustion and Flame 51, p.357, 1983.

Sterling, A., 1987, private communication.

Street, J.C., and Thomas, A., "Carbon Formation in Premixed Flames," Fuel 34, p.4, 1955.

Takahashi, F., and Glassman, I., "Interpretation of Sooting Correlations under Premixed Conditions," 1982 Technical Meeting, the Eastern Section of the Combustion Institute Meeting, Paper No. 56, 1982.

Tesner, P.A., Snergiriova, T.D., and Knorre, V.G., "Kinetics of Dispersed Carbon Formation," Combustion and Flame 17, p.253, 1971.

Thomas, A., "Carbon Formation in Premixed Flames," Combustion and Flame 6, p.46, 1962.

Van de Hulst, H.C., Light Scattering by Small Particles Dover Pub., New-York, 1981.

Vinckier, C., Gardner, M.P., and Bayes, K.D., "A Study of Some Primary and Secondary Chemi-Ionization Reactions in Hydrocarbon Oxidations," S16th Symposium (Int.) on Combustion, the Combustion Institute, Pittsburgh, p.81, 1977.

Wagner, H. Gg., "Soot Formation - An Overview," in Particulate Formation During Combustion (Siegla, D. C., and Smith, G. W., ed.), Plenum Press, New-York, p.1, 1981.

Wang, T.S., Matula, R.A., and Farmer, R.C., "Combustion Kinetics of Soot Formation from Toluene,"18th Symposium (Int.) on Combustion, the Combustion Institute, Pittsburgh, p.1149, 1981.

Wey, C., Powell, E.A., and Jagoda, J.I., "The Effect of Temperature on Soot Formation in a Gaseous Diffusion Flame," in Chem. Phys. Processes in Combust., paper 7, p.4, Atlanta, GA., 1982.

Wersborg, B.L., Howard, J.B., and Williams, G.C., "Physical Mechanisms in Carbon Formation in Flames," 14th Symposium (Int.) on Combustion, the Combustion Institute, Pittsburgh, p.929, 1973.

Wersborg, B.L., Yeung, A.C., and Howard, J.B., "Concentration and Mass Distribution of Charged Species in Sooting Flames," 15th Symposium (Int.) on Combustion, the Combustion Institute, Pittsburgh, p.1439, 1975.

Wittig, S.L.K., Lester, T.W., in Evaporation-Combustion of Fuels (J.T. Zung, ed.), American Chemical Society, Advances in Chemistry Series 166, Washington, D.C., p.167, 1978.

BIOGRAPHICAL SKETCH

Abderrahmane Touati was born on January 27, 1955, in Algiers, Algeria. He received an engineering degree in petrochemical engineering from the Algerian Institute of Petroleum in 1980. After working for one year with an Algerian Petroleum Company, he was a recipient of a 3 year scholarship to study in the United States. He received the degree of Master of Science in mechanical engineering at the University of Florida in August 1983 and started the Ph.D. program in Fall 1983.

I certify that I have read this study and that in my opinion it conforms to acceptable standards of scholarly presentation and is fully adequate, in scope and quality, as a dissertation for the degree of Doctor of Philosophy.

Charles L. Proctor, II, Chairman
Associate Professor of Mechanical Engineering

I certify that I have read this study and that in my opinion it conforms to acceptable standards of scholarly presentation and is fully adequate, in scope and quality, as a dissertation for the degree of Doctor of Philosophy.

Alex E. Green
Graduate Research Professor of Mechanical Engineering

I certify that I have read this study and that in my opinion it conforms to acceptable standards of scholarly presentation and is fully adequate, in scope and quality, as a dissertation for the degree of Doctor of Philosophy.

John R. Eyler
Associate Professor of Chemistry

I certify that I have read this study and that in my opinion it conforms to acceptable standards of scholarly presentation and is fully adequate, in scope and quality, as a dissertation for the degree of Doctor of Philosophy.

Roger A. Gater
Associate Professor of Mechanical Engineering

I certify that I have read this study and that in my opinion it conforms to acceptable standards of scholarly presentation and is fully adequate, in scope and quality, as a dissertation for the degree of Doctor of Philosophy.

William E. Lear, Jr.
Assistant Professor of Mechanical Engineering

This dissertation was submitted to the Graduate Faculty of the College of Engineering and to the Graduate School and was accepted as partial fulfillment of the requirements for the degree of Doctor of Philosophy.

August 1987

Dean, College of Engineering

Dean, Graduate Scool